

Modified Hydroxyapatite Coating on Stainless Steel Substrate for Orthopedic Implants



**By
Aysha Awan**

**School of Chemical and Materials Engineering
National University of Sciences and Technology**

2023

Modified Hydroxyapatite Coating for Orthopedic Implants



Name: Aysha Awan

Reg.No: 00000320740

**This thesis is submitted as a partial fulfillment of the requirements for
the degree of**

MS in (Materials & Surface Engineering)

Supervisor Name: Dr. -Ing. Farhan Javaid

Co. Supervisor Name: Dr. Usman Liaqat

School of Chemical and Materials Engineering (SCME)

National University of Sciences and Technology (NUST)

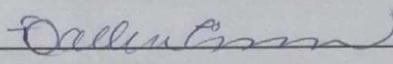
H-12 Islamabad, Pakistan

August,2023



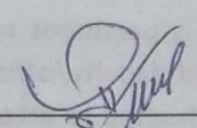
THESIS ACCEPTANCE CERTIFICATE

Certified that final copy of MS thesis written by Ms **Aysha Awan** (Registration No 00000320740), of School of Chemical & Materials Engineering (SCME) has been vetted by undersigned, found complete in all respects as per NUST Statues/Regulations, is free of plagiarism, errors, and mistakes and is accepted as partial fulfillment for award of MS degree. It is further certified that necessary amendments as pointed out by GEC members of the scholar have also been incorporated in the said thesis.

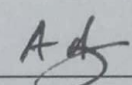
Signature: 

Name of Supervisor: Dr Farhan Javed

Date: 29 - Aug - 2023

Signature (HOD): 

Date: 31/08/2023

Signature (Dean/Principal): 

Date: 4.9.2023



Form TH-1
(Must be type written)

National University of Sciences & Technology (NUST)

MASTER'S THESIS WORK

Formulation of Guidance and Examination Committee (GEC)

Name: Aysha Awan

NUST Reg No: 320740

Department: SCME

Specialization: MS Materials and surface engineering

Credit Hour Completed: 24

CGPA: 3.06

Course Work Completed

S/No	Code	Title	Core/Elective	CH	Grade
1	MSE 854	Characterization of materials	elective	3	B+
2	MSE 821	Mechanical behavior of materials	core	3	B
3	MSE 811	Materials thermodynamics	core	3	C
4	MSE 861	Engineering ceramics and glasses	elective	3	B
5	MSE 812	Phase transformation & microstructures	core	3	B
6	MSE 851	Surface engineering & characterization	core	3	B+
7	MSE 852	Advance surface coatings	elective	3	B
8	MSE 881	Manufacturing processes	elective	3	B+

Date: 28 October 2021

Student's Signature: Aysha

Thesis Committee

- Name: Dr. Farhan Javaid (Supervisor)
Department: SCME, NUST
- Name: Dr. Usman Liaqat (Co-Supervisor)
Department: SCME, NUST
- Name: Dr. Zakir Hussain
Department: SCME, NUST
- Name: Dr. M. Aftab Akram
Department: SCME, NUST
- Name: _____ (External)
Department: _____

Signature: [Signature]
Signature: [Signature]
Signature: [Signature]
Signature: [Signature]
Signature: _____

Date: _____

Signature of Head of Department: [Signature]

APPROVAL

Date: 9.11.2021

[Signature]
Dean/Principal

Distribution

- 1x copy to Exam Branch, Main Office NUST
- 1x copy to PGP Dte, Main Office NUST
- 1x copy to Exam branch, respective institute

School of Chemical and Materials Engineering (SCME) Sector H-12, Islamabad



National University of Sciences & Technology (NUST)

FORM TH-4

MASTER'S THESIS WORK

We hereby recommend that the dissertation prepared under our supervision by

Regn No & Name: 00000320740 Aysha Awan

Title: Modified Hydroxyapatite coating on stainless steel substrate for orthopedic implants.


Presented on: 28 Aug 2023

at: 1100 hrs in SCME Seminar Hall

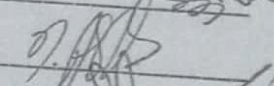
Be accepted in partial fulfillment of the requirements for the award of Masters of Science degree in **Materials & Surface Engineering.**

Guidance & Examination Committee Members


Name: Dr Zakir Hussain

Signature: 

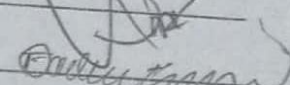
Name: Dr Muhammad Aftab Akram

Signature: 

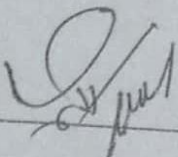
Name: Dr Usman Liaqat Co-Supervisor)

Signature: 

Supervisor's Name: Dr Farhan Javaid

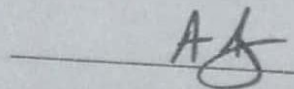
Signature: 

Dated: 28 AUG 2023



Head of Department

Date 29/8/23



Dean/Principal

Date 29.8.23

Dedication

To my beloved parents, husband and friends for their love, support, and motivation.

Acknowledgement

Praise be to Allah Almighty, who provided guidance and fortitude at each juncture of my research endeavors and bestowed upon me the resilience necessary to bring it to fruition. I express my gratitude to my cherished family and friends for their unrelenting support, encouragement, and affection throughout my efforts. I extend my profound appreciation to my supervisor, co-supervisor, GEC members & SCME for their distinguished oversight, priceless counsel, and direction.

Aysha Awan.

Reg No. 00000320740.

Abstract

In recent years, Hydroxyapatite (HAp) has garnered significant attention from researchers in the biomedical field. To emulate natural bone appetite, various combinations of elements are being utilized for substitution within the Hydroxyapatite lattice. In this study, HAp, and modified Hydroxyapatite (by substituting Sr^{2+} , Mg^{2+} , and Ag^+ ions) powders were synthesized via wet precipitation method and then coated onto stainless steel (SS 316L) through spin coating. The XRD and FTIR analyses confirmed the formation of HAp and modified HAp. For the characteristic HAp XRD peaks, e.g., for (211), a peak shift from 31.7 to 30.9 with peak broadening was also observed. The FTIR analysis also shows the HAp characteristic absorption spectra for $-\text{OH}$, CO_3^{2-} , PO_4^{3-} and HPO_4^{2-} groups at 3400 cm^{-1} to 3600 cm^{-1} with specific peak at 3570 cm^{-1} , 1400 cm^{-1} to 1650 cm^{-1} , 560 cm^{-1} to 650 cm^{-1} and 1040 cm^{-1} respectively. Moreover, a peak broadening for $-\text{OH}$ and CO_3^{2-} groups were observed after the substitution of Sr^{2+} , Mg^{2+} , and Ag^+ ions. The morphology of the prepared powdered samples was studied using Scanning Electron Microscopy (SEM). For the HAp and modified HAp powdered samples, the SEM analysis shows agglomerated particles with approximate round and flaky shapes, respectively. For the measurement of coating thickness of modified HAp, a few cross-sections were prepared, and the SEM analysis confirmed a dense and uniform coating with a thickness of $100 \pm 2\ \mu\text{m}$. The surface roughness of modified HAp was $2.35 \pm 0.02\ \mu\text{m}$ which was observed using optical profilometry. Corrosion resistance testing results were obtained using three electrode cell assembly via Gamry (potentiostat) in which R_p value increase from 71.92×10^3 to 174.7×10^3 , whereas corrosion rate decreases from 6.846 Mpy to $284.9 \times 10^{-3}\text{ Mpy}$, and antibacterial properties of the prepared samples were investigated using disc diffusion method. The results of the modified HAp coating samples show improved antibacterial, corrosion, and surface properties, unequivocally highlighting their potential as ideal candidate for orthopedic implant.

Table of Contents

1	Introduction	1
1.1	Biomedical devices:.....	1
1.2	Orthopedic implants:.....	3
1.3	Types of materials: Metal, Polymer, Ceramic and Composites.	4
1.3.1	Metals:	4
1.3.2	Ceramics and glasses:.....	5
1.3.3	Polymers:	6
1.3.4	Composites:	7
1.4	Research problem:	7
1.5	Objectives:.....	13
2	Literature review.....	14
2.1	Hydroxyapatite:	14
2.1.1	Chemical composition of Hap:	14
2.1.2	Reason of selecting Hydroxyapatite:.....	14
2.1.2.1	Biocompatibility:	15
2.1.2.2	Bioactivity:	15
2.1.2.3	Osteo-conductivity:	15
2.1.2.4	Structural Similarity to Bone:	15
2.1.2.5	Mechanical Compatibility:	15
2.1.2.6	Slow Degradation Rate:.....	15
2.1.3	Synthesis of HAp.....	16
2.1.3.1	Wet chemical precipitation:	16
2.1.3.2	Sol-gel method:.....	16
2.1.3.3	Biomimetic Mineralization:.....	16
2.1.3.4	Hydrothermal/Solvothermal Synthesis:	16
2.1.3.5	Electrochemical Deposition:.....	16
2.1.3.6	Electrophoretic deposition:.....	17
2.1.4	Modification in hydroxyapatite lattice:	17
2.1.4.1	Single cationic substitutions:	17
2.1.4.2	Co-substitutions in hydroxyapatite:	20
2.2	Stainless Steel 316 L:.....	20

2.2.1	Properties of SS 316 L as orthopedic implant:	20
2.2.2	Mechanical properties of steel	21
2.2.3	Coating methods:	22
2.2.3.1	Physical vapor deposition:.....	22
2.2.3.2	Sputter Deposition:.....	22
2.2.3.3	Thermal Evaporation:.....	22
2.2.3.4	Pulsed laser deposition (pld):.....	23
2.2.3.5	Dip coating:	23
2.2.3.6	Sol-gel coating:	23
2.2.3.7	Spin coating:	23
2.2.3.8	Electroplating/electrodeposition:	24
3	Experimental work.....	25
3.1	Synthesis of hydroxyapatite (HAp):	25
3.1.1	Materials & method:.....	25
3.2	Synthesis of modified hydroxyapatite (M1):	26
3.2.1	Materials & method:.....	26
3.3	Synthesis of modified hydroxyapatite (M2):	27
3.4	Substrate preparation:	28
3.5	Coating on Stainless Steel 316 L:.....	28
3.6	Characterization:.....	28
3.6.1	X-Ray Diffraction:	28
3.6.2	Fourier Transform Infrared Spectroscopy (Powder):.....	30
3.6.3	Scanning Electron Microscope:	33
3.6.4	Energy dispersive X-ray (EDX):.....	35
3.6.5	Corrosion testing (Coated sample):.....	35
3.6.5.1	Open circuit potential:	35
3.6.5.2	Electrochemical Impedance Spectroscopy:	36
3.6.5.3	Potential-dynamic polarization:.....	36
3.6.6	Optical Profilometry:.....	37
3.6.7	Contact angle:	37
3.6.8	Antibacterial testing:	38
4	Results & Discussions.....	41
4.1	X- Ray Diffraction Analysis:	41
4.2	FT-IR Analysis:	44

4.3	Scanning Electron Microscopic Analysis:	45
4.4	Corrosion Testing:	46
4.5	Anti-bacterial Testing:	48
4.6	Optical Profilometry:	50
4.7	Contact Angle:.....	51
4.8	Conclusion:.....	51
	References	53

List of Figures

Figure 1 Medical devices [4].....	2
Figure 2 foot amputation [9]	2
Figure 3 Buddy method for finger fracture [12].....	4
Figure 4 Hip implant [14]	5
Figure 5 Hydroxyapatite coating on dental implant [14]	6
Figure 6 Polymeric and composite based implants [22]	7
Figure 7 Structure of Hydroxyapatite [25].....	8
Figure 8 Strontium effect while bone formation [27].....	9
Figure 9 Magnesium role in bone (Biomineralization) [30].	10
Figure 10 Silver nanoparticles reaction with bacteria [31]	11
Figure 11 SS 316 L microstructure [33].	11
Figure 12 Corrosion in SS 316 L hip implant [34]	12
Figure 13 HAp synthesis Schematic	26
Figure 14 Modified HAp synthesis schematics.....	27
Figure 15 Bragg's law schematic illustration [71].	29
Figure 16 X Ray spectrometer schematic [72].	30
Figure 17 FTIR instrumentation [74].....	31
Figure 18 SEM Instrumentation [75].	33
Figure 19 electron emission from sample in SEM [76].	34
Figure 20 young's equation and contact angle representation [83].	38
Figure 21 XRD of HA, M1 & M2	41
Figure 22 major peaks of HAp, M1 & M2.....	42
Figure 23 Zoomed in XRD to show peak shift.....	43
Figure 24 XRD of (a) HAp coated SS & (b) Modified HA coated SS.....	44
Figure 25 FTIR of HA, M1 & M2	44
Figure 26 SEM images of (a) HAp, (b) M2	45
Figure 27 SEM image of cross-section of coated SS 316 L with M2	46
Figure 28 Nyquist plot of SS 316L & M2.....	47

Figure 29 Potentiodynamic polarization curves of SS 316L & M2 48
Figure 30 Agar disc diffusion test. 49
Figure 31 (a)M2 coated SS (b) bare SS surface. 51

List of Tables

Table 1 Amount of materials used in synthesis.....	25
Table 2 Potentio-dynamic polarization results	47

List of Abbreviations:

Abbreviation	Description
HAp	Hydroxyapatite.
M1	Modified Hydroxyapatite (Ag > Mg).
M2	Modified Hydroxyapatite (Mg > Ag).
Sr ²⁺	Strontium ion.
Mg ²⁺	Magnesium ion.
Ag ⁺	Silver ion.
Ca ²⁺	Calcium ion.
pH	Power of hydrogen.
DI water	De Ionized water.
Ca (OH) ₂	Calcium hydroxide.
H ₃ PO ₄	Phosphoric acid.
Mg (OH) ₂	Magnesium hydroxide.
PEEK	Poly ether ether ketone.
KU PEKK	Kumovis poly ether ketone ketone.
PGA	Polyglycolic acid.
PLA	Polylactic acid.
JCPD	Joint committee on powder diffraction standards.
Mpy	Mils per year.
OCP	Open circuit potential.
EIS	Electrochemical impedance spectroscopy.

Chapter: 1

1 Introduction

In recent times a lot of research has been conducted on materials that are biologically compatible [1]. Now, in addition to providing support to the bone, materials can also aid in the augmentation of the healing process. For instance, in the case of orthopedic fractures, such materials are utilized which facilitate bone growth while simultaneously providing support to the fractured bone. In previous times, the utilization of a solitary material, for instance, steel or titanium, was customary as an implant. However, the advancement in the medical domain has facilitated the application of diverse materials as implants, including titanium alloys, polymers, ceramics and so forth [2].

1.1 Biomedical devices:

An item, device, contrivance, or mechanism utilized for the purpose of averting, identifying, or addressing maladies or disorders, or for ascertaining, quantifying, rehabilitating, rectifying, or adapting the configuration or activity of the physique for the sake of promoting health [3]. These can be complex or simple such as tongue depressor, thermometer, pacemaker, dental implant etc. [4]. Some of these devices are shown in Figure 1. These devices should possess some fundamental properties like biologically inert or biofriendly. A wide range of biological devices are used in the medical field today [5-7]. Their choice of material, crystal structure, chemical and physical properties all depend on application. Such as for orthopedic implants we need properties like strength, durability, wear resistance etc. While the thread used for stitches should be flexible and degradable in body.

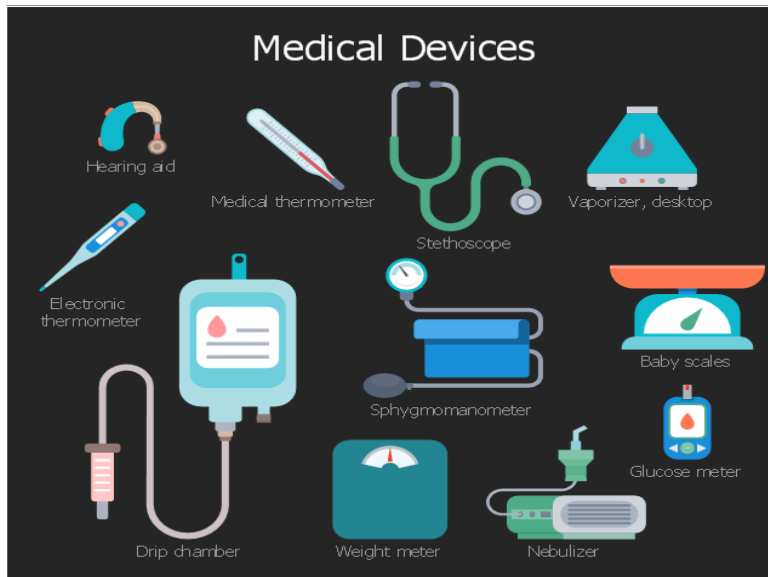


Figure 1 Medical devices [4]

History and significance of biomaterials:

In the beginning of the medical field there was much less understanding of tissues and cell regeneration. In most cases if any body part gets damaged there were only two methods: mostly used one is to completely replace the damaged part and second was to use insert piece of any material in place of damaged body part like a glass eye if eye gets damaged [8].



Figure 2 foot amputation [9]

Figure 2 illustrates a severely fractured leg [9], necessitating foot amputation as the sole viable option. However, given the recent advancements in biological knowledge, disease pathology, and tissue function, there has been renewed interest in the repair of damaged tissues. Currently, tissue regeneration has become a feasible prospect through the utilization of cell-based tissue engineering. Biomaterials notion has evolved with time in 1987 Williams defined it as “A biomaterial refers to an inanimate substance utilized in medical appliances with the purpose of engaging with biological systems”[8, 10]. This definition stands true for previous use of biomaterials as well as its current use but there is a huge difference in understanding of biomaterials in previous era, they are supposed to be biologically inert while in current date and time they are supposed to interact with biological system i.e., Human body. Such biomaterials are now available that help the body to start tissue regeneration, help in cell adhesion and maybe in future we can regenerate a full organ through stem cells. As cell and tissue interaction with biomaterials is so complex it will be beneficial to seek help from nature while choosing suitable material and its preparation mechanism this approach is known as biomimetics. In this approach researchers try to incorporate properties of natural materials or living tissues their chemical aspect structure and preparation method [11]. The needs of properties of biomaterials also varies according to the application of them in human body so it must be kept in mind too.

1.2 Orthopedic implants:

Since the stone age people have been getting bone fractures and treating them through different methods. Some of them are still being used like the buddy method [12] if fracture is in finger as illustrated in Figure 3. Some fractures were treated by tying wooden sticks around to give support to the bone, but as medical science developed, techniques for treating fractures also improved.



Figure 3 Buddy method for finger fracture [12].

Many types of implants are being used now a days some of them are permanent while some are temporary according to the need of patient [13]. Metallic materials are commonly used as orthopedic implants such as stainless steel, titanium alloys, cobalt-based alloys, biodegradable alloys etc. They are used due to their properties i.e., strength, fracture toughness, hardness, ductility etc. These materials are used routinely as orthopedic implants and are approved by US food and drugs administration.

1.3 Types of materials: Metal, Polymer, Ceramic and Composites.

Wide variety of materials can be used as biomaterials for any biomedical application. First, an engineer should select a general class of material to use from the four primary classes of materials i.e., metals, polymers, ceramics, and composites (mixture of any first three classes of materials).

1.3.1 Metals:

Biomaterials made up of metals are highly used. Due to their properties, they are a good fit for implants. Biomaterials made of metals can be categorized in three groups:

Iron-based alloys, cobalt-based alloys, and titanium-based alloys [8]. Figure 4 illustrates a total hip implant made up of metal [14].



Figure 4 Hip implant [14]

Metallic implants are used in orthopedic and dental field due to their high strength, corrosion resistance, wear resistance etc. We can remove broken bones or joints and replace it with orthopedic implants such as hip or knee implants can be temporary too, which assist bone regeneration such as plates screws and rods. Selection of material depends upon many factors, and one should consider each property needed for the application [11].

1.3.2 Ceramics and glasses:

There are many pros and cons of this class of materials but it all boils down to the application. Advantages of these materials are that they are highly biocompatible, does not react in body, they resist deformation during compression, they don't offer breeding ground for bacteria but their properties like brittleness, sudden fracture without any plastic deformation are some disadvantages [15].



Figure 5 Hydroxyapatite coating on dental implant [14]

Few examples of ceramics are hydroxyapatite as shown in Figure 5 , alumina, zirconia etc. [2, 16]. The atomic structure of these materials is very different from metals. Atomic bonds are weak and atoms are mobile in metals whereas in ceramics ionic and covalent bonds are present and atoms are not mobile that make them bad conductor of heat and electricity too [17]. Glass has amorphous structure they are mostly silica based. Silica forms bonds in a network form. Ceramics have a higher melting temperature than metals usually above 1000°C [18].

1.3.3 Polymers:

These are materials made up of very large molecules composed of regularly repeating small units. They are suitable for biomedical applications due to their wide range of properties, and they also replicate naturally occurring materials like proteins and nucleic acid etc. [19]. Slight changes in chemical composition can make polymer rigid or flexible, low or highly strengthened. Surface modification also impacts their interaction with the body i.e., they can resist attachment with protein, or they can encourage protein attachment [8]. Some polymers are biodegradable, and some are permeant depending on their synthesis. They are usually used as an intermediate layer between implant surface and bone. These properties can be proven beneficial or fatal so characterization of polymer before and after implantation is a vital step while making a biomedical device

[20]. Polymer implant consisting of Polyether ether ketone (PEEK), Kumovis Polyether ketone ketone (KU PEKK), etc. is used as midfacial implant in place of usually used titanium implant because titanium local magnetic field interferes with external magnetic field of machines like CT scan [21]. Sutures used in orthopedic implants are also made up of polymers such as Absorbable polyglycolic acid (PGA), polylactic acid (PLA), etc. [20]. These polymers show high tensile strength, less elongation, and high modulus that make them perfect for their application [22]. Some examples are also shown in Figure 6.

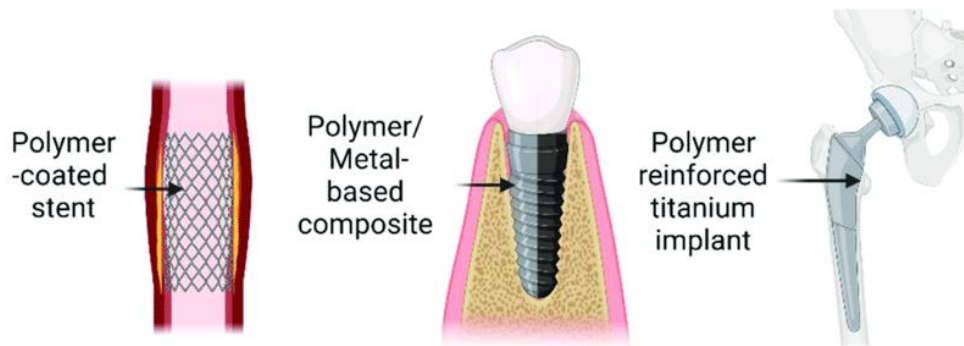


Figure 6 Polymeric and composite based implants [22]

1.3.4 Composites:

Composites are materials that are a combination of metals, polymers, ceramics, or glasses. Some composites that are composed of ceramics and glass have shown to be promising for the direct bone bonding which is vital in permanent orthopedic implants. Some of the examples of composites are zirconia toughened alumina, alumina toughened zirconia and strontium hexa aluminate used in total hip replacement ball heads, humeral head in shoulder replacement [23] etc. By mixing these composites we can retain intrinsic properties of ceramic and enhance properties like fracture toughness and strength.

1.4 Research problem:

Hydroxyapatite is naturally present in bones and teeth, but it is amorphous, calcium deficient and carbonated. Hydroxyapatite synthesized in labs is crystalline and have Ca/P 1.67 ratio [24]. Structure of hydroxyapatite [25] is shown in Figure 7. As

synthesized hydroxyapatite is chemically very close to naturally occurring hydroxyapatite it shows promising behavior with bones when it comes to bonding.

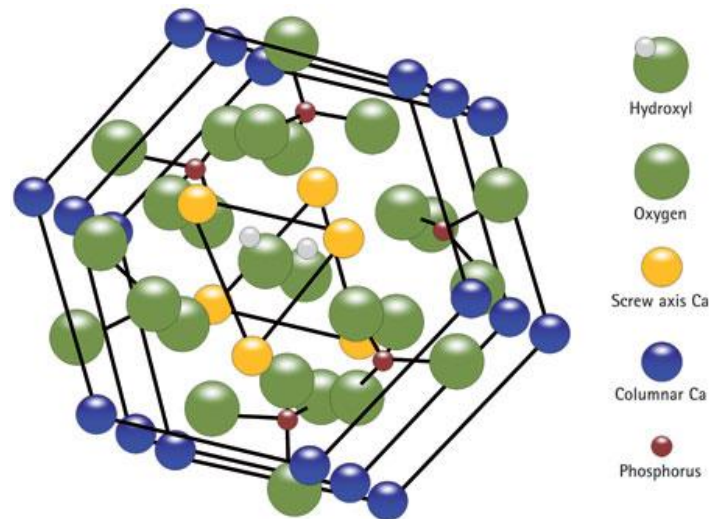


Figure 7 Structure of Hydroxyapatite [25].

However, the employment of pure hydroxyapatite is restricted due to its biocompatibility and degradation rate limitations [26]. By introducing specific ions into the HA structure, the biocompatibility of the material can be enhanced, thereby facilitating more effective assimilation with adjacent tissues, and encouraging osteogenesis. Substituting elements can serve to boost the mechanical features of hydroxyapatite. To illustrate, introducing magnesium (Mg) or strontium (Sr) ions through substitution can augment the fracture toughness and flexural strength of HA, rendering it more resilient to stress-induced cracking or fracturing. The control of hydroxyapatite degradation can be achieved through ion substitution, a crucial aspect in scenarios where gradual degradation is required for the proper healing and integration of newly formed bone tissue. The inclusion of different elements in hydroxyapatite can bestow upon it bioactive and osteoinductive properties. For example, the incorporation of ions such as strontium or zinc can stimulate the formation of bone tissue and heighten osteoblast activity, which in turn accelerates and improves the process of bone regeneration. Elemental substitution presents an avenue for researchers to customize the characteristics of hydroxyapatite to cater to particular applications. By opting for diverse

ions for substitution, the formula, configuration, and traits of hydroxyapatite can be altered to meet varying biomedical purposes. We have chosen strontium, magnesium, and silver for ion substitution.

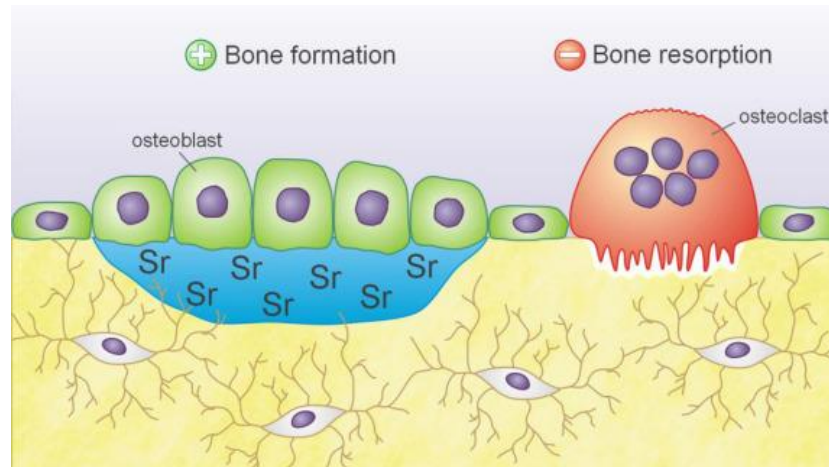


Figure 8 Strontium effect while bone formation [27].

The rationale behind the selection of strontium lies in its comparatively lesser ionic radius as compared to calcium, thus enabling the observation of lattice deformation in strontium-substituted hydroxyapatite. Significantly, the potential of strontium in ameliorating the condition of osteoporosis patients is evidenced by its marked effects on bone resorption, osteoblast, and osteoclast activity [27]. Effect of strontium [28] while bone growth is shown in Figure 8. Strontium doped hydroxyapatite showed promising effects on cell attachment and bone proliferation [29]. Hydroxyapatite substituted with strontium possesses the capability to serve as a viable repository of strontium, which can be effectively harnessed during the process of bone development.

Magnesium, an essential element, can be found within the human body. The adult human body contains approximately 25g of this vital element. Its properties are comparable to calcium regarding bone generation and cell membrane stabilization. Notably, its insufficiency can result in detrimental effects on both physical and mental abilities, with a particular emphasis on bone growth, bone density reduction, and bone fragility etc. [27].

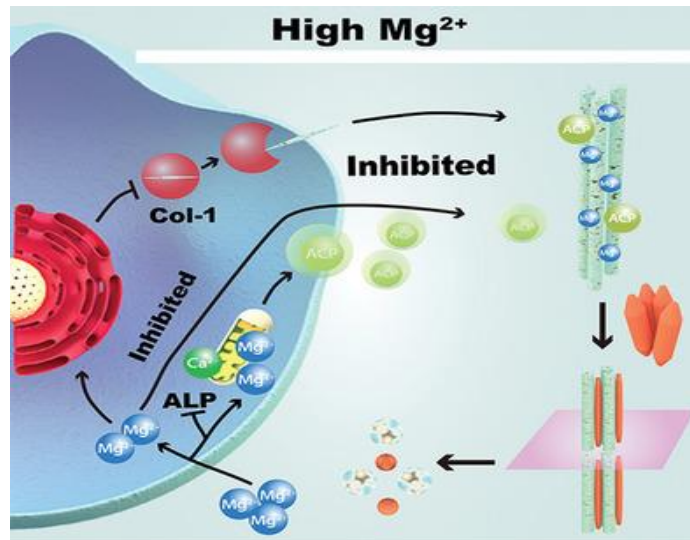


Figure 9 Magnesium role in bone (Biomineralization) [30].

Magnesium can be utilized as a substitute in hydroxyapatite, thereby rendering it more akin to bone apatite. Owing to its ability to impede the formation of large crystals, synthesized hydroxyapatite is rendered less crystalline, thereby facilitating the formation of a larger number of apatite nuclei. The presence of bone apatite assists in cell turnover, as well as osteoblast and osteoclast activity [30]. Magnesium interaction with bone cell [31] is demonstrated in Figure 9. Due to the above properties magnesium is selected for substitution.

Silver is not inherently present within the human body. However, the scientific community is significantly intrigued by the potential integration of silver into bio ceramics, primarily due to its exceptional antibacterial properties [27]. The inclusion of silver guarantees a reduced incidence of infection in bone or dental implants. The antimicrobial attribute of silver is attributed to its aptitude to interact with the DNA of microorganisms, thereby impeding bacterial proliferation [32].

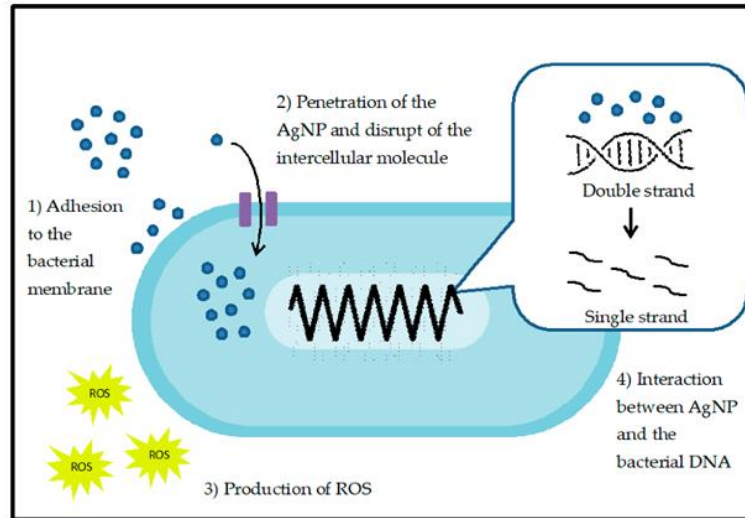


Figure 10 Silver nanoparticles reaction with bacteria [31]

This phenomenon is illustrated in Figure 10. The substitution of Ag in hydroxyapatite is an easily achievable task that can be applied to metallic implants. Silver ions also help in adhesion strength of coating on implant. The aforementioned attributes serve as the rationale behind selecting strontium, magnesium, and silver for the purpose of substituting in hydroxyapatite.

Metal substrates are used for their load bearing properties because metals possess better mechanical properties than ceramics. Different metal substrates can be used such as titanium, cobalt, iron, and their alloys. Stainless steel, an alloy composed of iron, is infused with a composition of chromium, nickel, molybdenum, and manganese alongside other trace elements is used as substrate material. Notably, stainless steel possesses a historical significance as one of the primary metals utilized for orthopedic

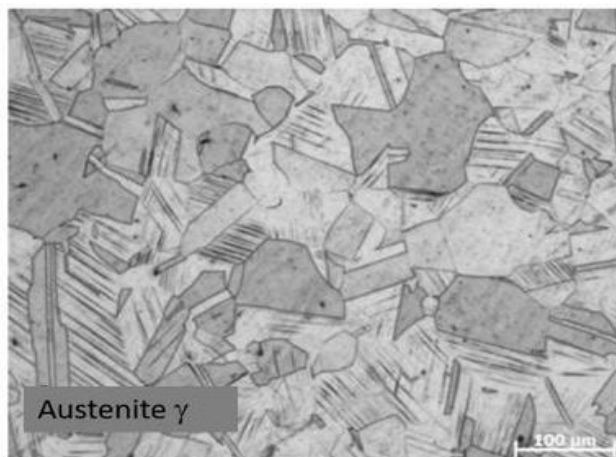


Figure 11 SS 316 L microstructure [33].

implants [33].

There are different types of stainless steel like SS 304, SS 316 L, SS 316 etc. We have chosen SS 316 L due to its low carbon content and high corrosion resistance due to presence of chromium, nickel, and molybdenum. Microstructure of SS 316 L [34] is shown in Figure 11. One of the limitations associated with stainless steel implants is their propensity to corrode over time when exposed to bodily fluids, leading to the development of bacterial infections.

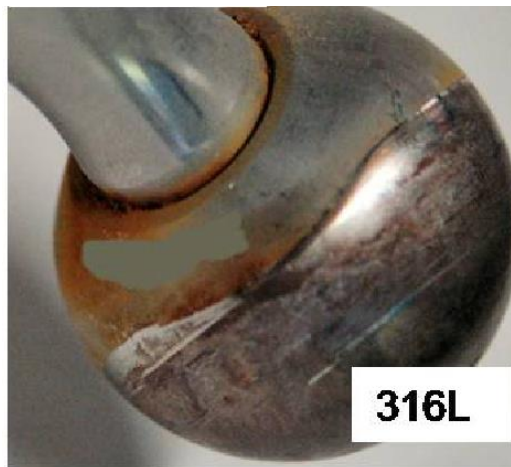


Figure 12 Corrosion in SS 316 L hip implant [34]

Figure 12 shows SS 316 L corrosion after being implanted in body [35]. Certain elements, such as nickel, cobalt, and chromium, are released within the body, subsequently entering the bloodstream, and ultimately depositing themselves within various organs. This process is known to contribute to a host of detrimental effects, including but not limited to kidney failure and blood poisoning. Hydroxyapatite, being inherently brittle, cannot withstand the demands of a load-bearing environment. As a result, when used in isolation, both SS 316L and hydroxyapatite prove to be unsuitable for orthopedic implants. To harness their respective properties and circumvent their shortcomings, a combination of these materials has been employed. Specifically, modified hydroxyapatite has been applied to surface-treated SS 316 L. This technique allows for the utilization of the load-bearing capabilities of steel, while the hydroxyapatite acts as a barrier between the steel and bodily fluids, thereby preventing corrosion and facilitating a surface conducive to bone growth.

1.5 Objectives:

The aims of our study are outlined below:

1. Synthesis of hydroxyapatite and modified hydroxyapatite with Sr^{2+} , Mg^{2+} , & Ag^+ ionic substitution.
2. Characterization of HAp and modified HAp powder through XRD, FT-IR, SEM and Antibacterial testing.
3. Coating of HAp and modified hydroxyapatite on SS316 L surface.
4. Characterization of coated SS 316 L through XRD, SEM, and Corrosion testing.
5. To get the improved surface, corrosion, and antibacterial properties of the modified HAp coating.

Chapter: 2

2 Literature review

This chapter will focus on antecedent studies that are pertinent to our undertaking. researchers shall peruse the biological and physical attributes of hydroxyapatite and stainless steel 316 L as employed in orthopedic implants. They shall expatiate on diverse hydroxyapatite production methodologies and deliberate on various hydroxyapatite coating approaches.

2.1 Hydroxyapatite:

The mineral calcium apatite has the chemical formula $\text{Ca}_{10}(\text{PO}_4)_6(\text{OH})_2$ and is found naturally as hydroxyapatite. It adds to the strength and hardness of vertebrate bones and teeth as the predominant inorganic component. Most of the mineralized matrix in bones is composed of hydroxyapatite crystals, which offer stiffness and structural support [36]. Due to its biocompatibility and resemblance to the mineral that makes up human bones, hydroxyapatite is frequently used in biomedical applications. It can be created in a lab and used in many ways, such as powders, coatings, and scaffolds. Such forms have uses in tissue engineering, dentistry, orthopedics, and drug delivery systems.

2.1.1 Chemical composition of Hap:

Hydroxyapatite shows hexagonal structure. The calcium ions (Ca^{2+}) in the hydroxyapatite lattice are encircled by phosphate (PO_4^{3-}) and hydroxide (OH^-) ions. Layers of calcium ions are present, and the spaces between the layers are filled by phosphate and hydroxide ions [37]. The distinctive qualities of hydroxyapatite, such as its high bioactivity and biocompatibility, are a result of its crystal structure.

2.1.2 Reason of selecting Hydroxyapatite:

Numerous studies on hydroxyapatite have been conducted to determine its qualities and benefits for use as an orthopedic implant [37]. Some of these characteristics are given below:

2.1.2.1 Biocompatibility:

Due to its good biocompatibility, hydroxyapatite is well tolerated by humans and does not have any negative effects. This characteristic is essential for orthopedic implants since it reduces the possibility of inflammation or rejection.

2.1.2.2 Bioactivity:

Hydroxyapatite has bioactive qualities. It can bind to living bone tissue directly. Osteointegration, the process by which an orthopedic implant merges with the surrounding bone, can be aided using HA in orthopedic implants. This increases the stability and durability of the implant.

2.1.2.3 Osteo-conductivity:

The capacity of HA to assist the formation and migration of bone cells (osteoblasts) onto the implant surface is known as high osteoconductive. This characteristic promotes the growth of new bone and its fusion with the implant, speeding up the healing process.

2.1.2.4 Structural Similarity to Bone:

Hydroxyapatite's chemical make-up and crystal structure are remarkably like those of bone material found in nature. This resemblance improves the implant's compatibility with the surrounding bone tissue, resulting in better long-term performance and a lower chance of problems.

2.1.2.5 Mechanical Compatibility:

Similar to genuine bone, hydroxyapatite is stiff and has a mechanical behavior. The stress shielding effects that can happen when there is a considerable mismatch in the mechanical characteristics of the implant and the surrounding bone are reduced thanks to this mechanical compatibility. HA implants can encourage more natural load transfer, reduce the risk of bone resorption, and implant loosening by minimizing stress shielding.

2.1.2.6 Slow Degradation Rate:

Because hydroxyapatite degrades slowly, its structural integrity can be preserved for a long time. This characteristic makes orthopedic implants more favorable since it protects the implant's durability and longevity while enabling normal bone healing and remodeling.

2.1.3 Synthesis of HAp

Depending on the desired form, size, and purity of the finished product, there are various ways to prepare hydroxyapatite [24, 38]. Here are a few typical approaches:

2.1.3.1 Wet chemical precipitation:

In the wet chemical precipitation process, calcium and phosphate precursors are combined in an aqueous solution at a regulated pH and temperature. Hydroxyapatite is created when the precursors react, and it can then be separated, cleaned, and dried [39, 40]. This approach is popular for laboratory-scale synthesis since it is reasonably straightforward.

2.1.3.2 Sol-gel method:

In this method, calcium and phosphate sources are dissolved in a solvent to create a precursor solution. A gel is created by the reaction of condensation and hydrolysis in the solution. The solvent is subsequently removed from the gel by heating it, which encourages further crystallization and produces hydroxyapatite [16, 41]. The purity, morphology, and composition of the finished product can all be controlled using the sol-gel process.

2.1.3.3 Biomimetic Mineralization:

This strategy imitates the biomineralization process, in which hydroxyapatite is created within organic matrices. It entails immersing a frame or template material in a solution called simulated body fluid (SBF), which replicates the ionic make-up of human plasma. On the scaffold surface, hydroxyapatite crystals form and increase over time, imitating the natural process of bone mineralization [42].

2.1.3.4 Hydrothermal/Solvothermal Synthesis:

This process includes heating and pressurizing a reaction mixture of calcium and phosphate precursors inside a closed vessel. The creation of nanosized particles is accelerated by the hydrothermal/solvothermal conditions, which also speed up the nucleation and growth of hydroxyapatite crystals [43]. Using this method, high-purity, crystalline hydroxyapatite with tailored particle size and shape can be produced.

2.1.3.5 Electrochemical Deposition:

Hydroxyapatite coatings can be applied to conductive substrates using electrochemical techniques. With this method, an electric current is applied while the substrate is

submerged in an electrolyte solution comprising calcium and phosphate ions [44]. Hydroxyapatite is formed on the substrate surface because of the deposition process, which is carried out via redox reactions.

2.1.3.6 Electrophoretic deposition:

Hydroxyapatite coatings or films are made using the electrophoretic deposition (EPD) process. A hydroxyapatite suspension is prepared, a deposition cell with a substrate and anode is set up, an electric field is applied, and the charged hydroxyapatite particles are allowed to migrate and deposit onto the substrate. The covered substrate is dried after deposition and may go through sintering [45]. The method, which is frequently utilized in biomedical and dental applications, allows control over the coating qualities.

2.1.4 Modification in hydroxyapatite lattice:

To increase the benefits of hydroxyapatite lattice over other materials for orthopedic implants, many types of substitutions can be used [27, 46]. Following is a list of some of them:

2.1.4.1 Single cationic substitutions:

Cationic substitution is the process of swapping out one kind of cationic species in a crystal lattice for another. A calcium phosphate mineral called hydroxyapatite (HAp) can go through cationic substitution to integrate different ions into its crystal structure. The most frequent cationic substitution in hydroxyapatite involves the interaction of calcium (Ca^{2+}) and other ions. Ionic doping is another name for this procedure, which has the potential to change the hydroxyapatite's bioactivity, mechanical toughness, and biocompatibility. The following are some instances of cationic substitution in hydroxyapatite:

Strontium (Sr^{2+}) substitution:

The development of strontium-substituted hydroxyapatite (Sr-HAp) results from strontium replacing calcium in the hydroxyapatite lattice. The potential of this alteration to enhance characteristics of hydroxyapatite and encourage bone regeneration has been researched [47, 48]. It has been demonstrated that strontium increases osteoblast activity and stimulates bone growth. The addition of strontium to HAp can encourage bone regrowth at the implant site, enhancing osseointegration and accelerating recovery.

1. Bone resorption is caused by osteoclast activity, which strontium has been proven to reduce. By inhibiting osteoclast activity and preserving bone density, strontium-substituted HAp can help prevent bone loss surrounding the implant.
2. Strontium substitution in HAp can improve the implant's mechanical qualities. The implant's stability and wear resistance can be improved by adding strontium ions, which can also boost the implant's hardness and compressive strength.
3. Strontium-substituted HAp has demonstrated antibacterial properties, reducing the risk of infection at the implant site. Strontium ions inhibit the growth of various bacteria, including common pathogens associated with implant-related infections.
4. The inflammatory response can be modulated by strontium, which has anti-inflammatory effects. Strontium added to ha implants can aid in reducing inflammation and fostering a more favorable environment for recovery.
5. Over time, strontium ions can be released under control from strontium-substituted ha. Long-term implant performance can be supported by the slow release of strontium, which can retain its favorable effects on bone remodeling and regeneration for a longer duration.
6. The body tolerates strontium-substituted HAp well and it has good biocompatibility. Strontium is incorporated into HAp without affecting its biocompatibility or ability to work with neighboring tissues [29, 49, 50].

Silver (Ag^+) substitution:

Due to the special qualities of silver, silver-substituted hydroxyapatite (Ag-HAp) has drawn interest for its possible use in orthopedic implants. Some of the advantages that are deduced from research in orthopedic implants made of silver-substituted hydroxyapatite have been discussed below:

1. Silver has significant antibacterial characteristics that make it effective against a variety of bacteria, fungi, and viruses. It can be continuously released locally by incorporating silver ions into hydroxyapatite, helping to avoid bacterial colonization and infection at the implant site, which are a major issue in orthopedic procedures. With less implant failure, and a better patient experience, this antimicrobial impact can help [32].

2. Silver ions have been shown to enhance osteoblast differentiation and proliferation, which aids in bone production and repair. Silver incorporated into hydroxyapatite may increase the osteogenic characteristics of the implant, promoting better bone fusion and implant stability [51].
3. Silver contains anti-inflammatory qualities that may be used to control the inflammatory reaction at the implant site. Ag-substituted hydroxyapatite implants may foster a more favorable healing environment and temper overactive immune responses by lowering inflammation [52].

Magnesium (Mg^{2+}) substitution:

The hydroxyapatite crystal structure can generate magnesium-substituted hydroxyapatite (Mg-HAp) when magnesium ions take the place of calcium ions. The crystallinity and rate of decomposition of hydroxyapatite can both be impacted by this replacement. The potential of Mg-HAp in bone tissue engineering applications has been investigated. The human body requires magnesium, a mineral that is involved in several biological processes. Because the presence of magnesium ions closely resembles the chemical makeup of bone, replacing magnesium in hydroxyapatite increases its biocompatibility. This lowers the possibility of negative reactions and improves how well the implant integrates with the surrounding bone tissue [53].

Magnesium has been discovered to stimulate osteoblast proliferation and differentiation, which results in greater bone production and quicker healing. Mg-HAp implants have the potential to promote bone development at the implant site, which will speed up osseointegration and increase the durability of orthopedic implants. The quantity of magnesium ions in hydroxyapatite can affect how quickly the substance degrades. Orthopedic implants must undergo controlled biodegradation for the implant to gradually transfer its load-bearing capability to the developing bone. By preserving a correct degradation rate, magnesium replacement ensures the mechanical stability of the implant throughout the healing process. Magnesium is said to have anti-inflammatory properties. Mg-HAp implants can control the inflammatory response at the implant site, reducing excessive inflammation and fostering an environment that is more conducive to recovery. The patient's recovery is accelerated, and postoperative problems are decreased thanks to this anti-inflammatory property [54, 55].

2.1.4.2 Co-substitutions in hydroxyapatite:

The simultaneous substitution of two or more distinct cations into the hydroxyapatite (HAp) lattice is referred to as co-substitution. This type of substitution can involve the replacement of calcium (Ca^{2+}) ions by multiple cations, resulting in a multi-element-substituted hydroxyapatite material. Co-substitution can alter the characteristics of ha and offer special functionalities for a variety of applications. Examples of co-substitutions in hydroxyapatite include the following:

Silver /magnesium substituted hydroxyapatite [56], strontium/ magnesium substituted hydroxyapatite [57], strontium/ silver substituted hydroxyapatite [58, 59], magnesium/ strontium/ zinc substituted hydroxyapatite [60], strontium, magnesium, sodium and florine substituted hydroxyapatite [61]. We can obtain the advantages of each element by co-substitution, and these replacements also make the hydroxyapatite lattice more amorphous, which is advantageous for our application.

2.2 Stainless Steel 316 L:

The term "316L stainless steel" refers to a particular kind of stainless-steel alloy. It is a version of the well-known stainless-steel grade 316L that has less carbon. The name is abbreviated "SS" for "stainless steel." A corrosion-resistant alloy with a high chromium content, usually between 10 and 20%, is stainless steel. Other alloying components like nickel, molybdenum, and occasionally reduced carbon content improve the material's mechanical characteristics and corrosion resistance [2].

2.2.1 Properties of SS 316 L as orthopedic implant:

There are many positive attributes of ss 316 l as orthopedic implants [8, 10, 62]. Some of them are listed below:

1. Corrosion Resistance: Excellent corrosion resistance is displayed by stainless steel 316L, especially in physiological settings. This is crucial for orthopedic implants since they spend a lot of time in contact with tissues and biological fluids. The implant's endurance and dependability are aided by its resistance to corrosion.
2. Low Carbon Content: As indicated by the "L" in 316L, this alloy has a lower carbon content than regular 316 stainless steel. The lower carbon concentration reduces

sensitization, which can result in corrosion and intergranular attack by forming chromium carbides.

3. **Biocompatibility:** Because SS 316L is biocompatible, the body tolerates it without any negative side effects or harmful effects. For orthopedic implants that come into touch with living tissues, it does not significantly cause immunological reactions or inflammation.
4. **High Strength:** The mechanical and high strength characteristics of SS 316L are well recognized. The ability to develop robust and long-lasting implant components that can endure the strains and pressures encountered in the human body is advantageous for orthopedic implants.
5. **Ease of Manufacturing:** SS 316L is easily fabricable into a variety of implant forms and sizes and is widely accessible. It can be machined, shaped, and welded, enabling the creation of customized implants to meet the demands of individual patients.
6. **Cost-Effectiveness:** SS 316L is an appealing option for orthopedic implants since it is relatively inexpensive as compared to some other implant materials, especially in situations where high-performance alloys are not required.
7. **Excellent Weldability:** Excellent weldability in stainless steel (SS) 316L makes it simple to weld and produce using standard welding methods like TIG (tungsten inert gas) or MIG (metal inert gas) welding.

2.2.2 Mechanical properties of steel

Tensile Strength: Tensile strength is the maximum amount of stress that a material can bear before breaking while enduring tension. SS 316 L has tensile strength ranging 485 to 620 megapascals. Since SS 316L has a high tensile strength, orthopedic implant applications can depend on it to endure imposed loads and pressures.

1. **Yield Strength:** SS 316L typically has a yield strength of between 170 and 310 mpa. The yield strength of a material is the stress at which it starts to deform permanently without breaking, or plastically. This characteristic is essential because it shows how well the material can withstand deformation under load.
2. **Elongation:** The usual range of elongation for SS 316L is between 40% and 60%. The ability of a substance to stretch or deform before breaking is known as

elongation. Higher elongation values suggest a material's stronger ductility and toughness.

3. **Modulus of Elasticity:** The elastic modulus, or Young's modulus, of stainless steel 316L is between 190 and 205 gigapascals (gpa). The material's stiffness or capacity to fend off elastic deformation is indicated by the modulus of elasticity. A stiffer material has a higher modulus of elasticity.
4. **Hardness:** On the Rockwell hardness scale (HRB), stainless steel 316L typically ranges in hardness from 70 to 90. Indentedal's resistance to being scratched or indented is measured by its hardness. SS 316L's capacity to withstand wear and resist surface damage is ensured by its hardness.

It is important to keep in mind that the mechanical characteristics of stainless steel 316L can change based on things like production procedures, heat treatments, and particular alloy compositions. These characteristics make SS 316L appropriate for structural components, orthopedic implants, and other devices that require high strength, corrosion resistance, and longevity.

2.2.3 Coating methods:

There are different coating methods which are used for coating on orthopedic implants. Some of them are as follows:

2.2.3.1 Physical vapor deposition:

Control over film thickness, composition, structure, and characteristics is possible with PVD processes. The target material intended film qualities, and specific requirements for the thin film or coating all influence the PVD technology that is selected.

2.2.3.2 Sputter Deposition:

With the help of high-energy ions, atoms from a target material are dislodged, and they then deposit onto a substrate to create a thin layer through the process called sputter deposition. The target material may have the same properties as the coating material or it may have distinct properties [63]. Sputter deposition can take many different forms, including reactive, magnetron, RF, and DC sputtering.

2.2.3.3 Thermal Evaporation:

To create vapor, thermal evaporation, sometimes referred to as electron beam evaporation, heats a source material in a vacuum. A thin film is created on a substrate by

the condensation of the vaporized atoms or molecules [64]. To reach the necessary temperature for vaporization, this method employs bombardment with electron beams or resistive heating.

2.2.3.4 Pulsed laser deposition (pld):

To create vapor, thermal evaporation, sometimes referred to as electron beam evaporation, heats a source material in a vacuum. A thin film is created on a substrate by the condensation of the vaporized atoms or molecules [65]. To reach the necessary temperature for vaporization, this method employs bombardment with electron beams or resistive heating.

2.2.3.5 Dip coating:

A substrate is coated by being dipped into a solution or suspension containing the coating material, which is then slowly removed. A thin coating material film forms on the substrate's surface as it is removed [66]. Dip coating is an easy, affordable process that works well for evenly coating items with complex geometries.

2.2.3.6 Sol-gel coating:

Through chemical reactions, a precursor solution or sol is transformed into a solid coating using the sol-gel coating techniques. Usually, the precursor solution contains metal alkoxides or inorganic salts that are hydrolyzed and condensed to produce a gel-like substance. The gel is then applied to the substrate and heated in order to drive the creation of a solid coating and eliminate the solvent [67, 68].

2.2.3.7 Spin coating:

Spin coating is a method for applying a thin coating or film on a flat substrate. A liquid solution or dispersion is applied to the substrate, and the substrate is quickly spun, causing the solution to spread and produce a thin, even coating. The procedure is carried out on a spin coater, a rotating platform with high-speed spinning capabilities. Centrifugal force causes the solution to be forced outward and distributed across the surface as the substrate spins. Simultaneously, the solvent in the solution quickly evaporates, leaving the coating material as a solid film in its place. Critical factors that affect the final film's thickness and shape are the spinning speed and time [69-71]. Due of its widespread application in several sectors, including as semiconductor production,

optoelectronics, and research simplicity, low cost, and capacity for controlled thickness production of homogenous thin films [48].

2.2.3.8 Electroplating/electrodeposition:

Utilizing an electrolytic cell to deposit a coating material onto a conductive substrate is known as electrodeposition or electroplating. This technique turns the substrate into the cathode while dissolving the coating material in an electrolyte solution. The coating material is reduced and deposited onto the substrate as a result of the application of an electric current [67].

Chapter: 3

3 Experimental work

Hydroxyapatite was prepared through wet precipitation method and modification in hydroxyapatite was done in two ratios named as M1 & M2. The amount of each salt added in each synthesis is discussed in the following Table 1

Table 1 Amount of materials used in synthesis

	Ca(OH) ₂	H ₃ PO ₄	Ag(NO) ₃	Mg(OH) ₂	Sr(NO ₃) ₂
HAp	0.92g	0.5ml			
M1	0.6853g	0.51317ml	0.2548g	0.04373g	0.21163g
M2	0.6853g	0.51317ml	0.08493	0.1093g	0.21163g

3.1 Synthesis of hydroxyapatite (HAp):

3.1.1 Materials & method:

Analytical grade Calcium hydroxide (Ca (OH)₂ ; AnalaR) and phosphoric acid (H₃PO₄ ; Sigma-Aldrich) were used as sources of calcium and phosphorus ions respectively. All the chemical compounds were employed in their as-received state, without any additional refinement or purification processes. A conical flask was placed on a hot plate set at 80°C with constant stirring. A magnetic stirrer was placed in a round bottom flask containing 25ml of de ionized (DI) water. 0.92g of Ca (OH)₂ was added in 25ml of DI water. Diluted H₃PO₄ was prepared in 100ml glass beaker by adding 0.5ml H₃PO₄ in 25ml DI water. Ca (OH)₂ solution was kept at 80°C for 1 hour with constant stirring. After 1-hour H₃PO₄ solution was added dropwise (1 to 2 drops per second) with burette while continuous stirring in Ca (OH)₂ solution. pH was examined through pH paper after addition of H₃PO₄ sol in Ca (OH)₂ sol. pH should be 7 to 7.5 if it is on the basic side, we add one drop of ammonia in the solution and wait for 5 to 10 mins. We kept adding 1 drop of ammonia after every 5 to 10 mins until 7 to 7.5 pH was attained. Solution was kept on stirring & heating for 1 hour at 80°C. After this the solution was kept for 24 hours to age. After 24 hours centrifugation was done of this solution at 4000 rpm for 20 mins. Heavy Particles sit at the bottom of centrifuge tubes and above solvent was

discarded. These obtained particles are then washed 3 times using DI water through centrifugation at 4000 rpm for 15 mins each. These washed particles are then transferred into a beaker or Petry dish and kept overnight in drying oven at 100°C. Obtained dried product was grinded with mortar and pastel to turn it into fine powder. Obtained powder was desired hydroxyapatite. Above process is illustrated in Figure 13.

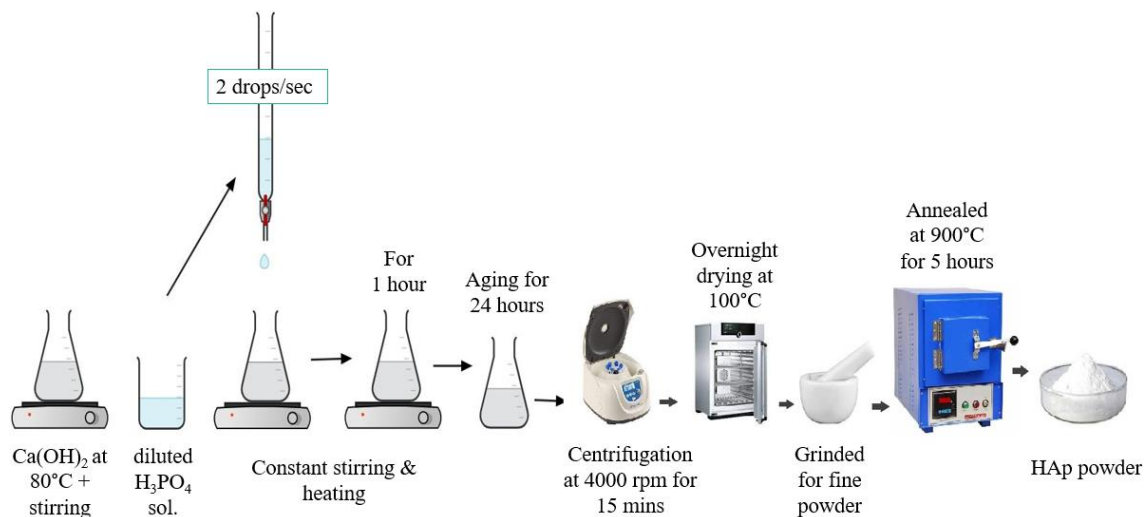


Figure 13 HAp synthesis Schematic

3.2 Synthesis of modified hydroxyapatite (M1):

3.2.1 Materials & method:

Analytical grade calcium hydroxide ($\text{Ca}(\text{OH})_2$; AnalarR) magnesium hydroxide ($\text{Mg}(\text{OH})_2$; AnalarR), silver nitrate ($\text{Ag}(\text{NO}_3)_3$; AnalarR), strontium nitrate ($\text{Sr}(\text{NO}_3)_2$; AnalarR) and phosphoric acid (H_3PO_4 , Sigma-Aldrich) were used as sources of calcium (Ca^{2+}), magnesium (Mg^{2+}), silver (Ag^+), strontium (Sr^{2+}) and phosphorous (P^{5+}). All the chemical compounds were employed in their as-received state, without any additional refinement or purification processes. Five solutions were formed. In $\text{Ca}(\text{OH})_2$ solution (Sol. 1), 0.6853g $\text{Ca}(\text{OH})_2$ was dissolved in 25ml Di water. In $\text{Mg}(\text{OH})_2$ solution (Sol. 2), 0.04373g $\text{Mg}(\text{OH})_2$ was dissolved in 25ml Di water. In $\text{Ag}(\text{NO}_3)_3$ solution (Sol. 3), 0.2548g silver nitrate was dissolved in 25ml Di water. In $\text{Sr}(\text{NO}_3)_2$ solution (Sol. 4), 0.21163g strontium nitrate was dissolved in 25ml Di water. In H_3PO_4 solution (Sol. 5), 0.51317ml of phosphoric acid was added in 25ml Di water. Solution 1 was kept on hot plate at 80°C with continuous stirring. Solution 2,3 and 4 were added in solution 1 after 30mins interval each on continuous heating and stirring. The resulting solution was

continuously stirred and heated for 30 mins. Solution 5 was poured in a burette which was adjusted on top of conical flask having above made solution. It was added dropwise (2 drops per sec) with continuous stirring and heating. When all solutions 1 to 5 were mixed properly the pH was examined, which should be 7 to 7.5. If the pH is on basic side, ammonia was added drop wise (1 drop per 5 mins) until pH comes down to 7 or 7.5. This solution was left stirring with continuous heating for an hour. After this we let prepared solution age for 24 hours. After 24 hours the solution was centrifuged at 4000rpm for 20 mins and the particles obtained at the bottom of centrifuge tube were washed thrice at 4000 rpm for 15 mins each with Di water via centrifugation. A paste like consistency was obtained which was then transferred into a beaker and kept in drying oven at 100°C overnight. Obtained dried product was grinded with mortar and pastel to turn it into fine powder. This was our required product. Above process is illustrated in Figure 14.

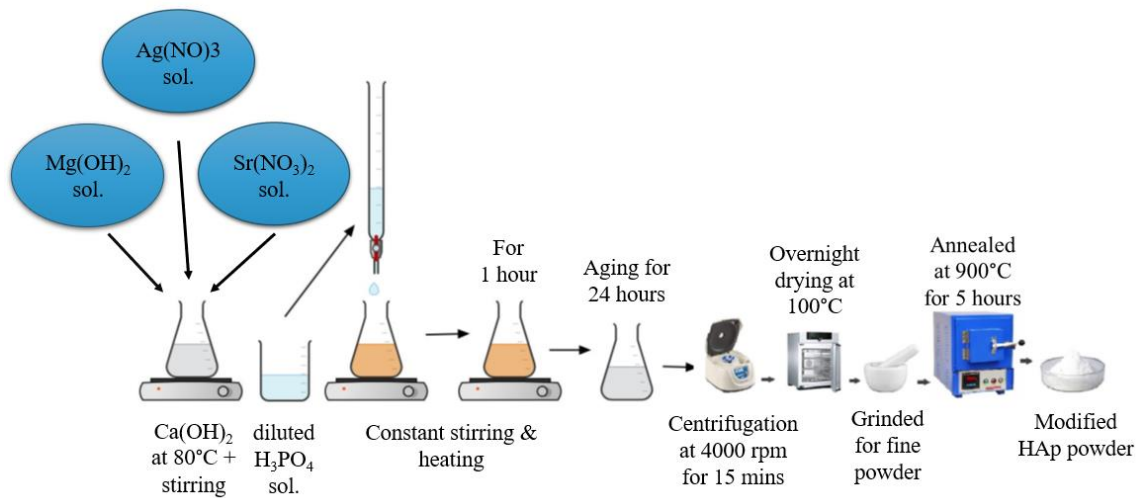


Figure 14 Modified HAp synthesis schematics.

3.3 Synthesis of modified hydroxyapatite (M2):

Synthesis of M2 was exactly like synthesis of M1 just the amount of silver nitrate and magnesium hydroxide was changed from 0.2548g and 0.04373g to 0.08493g and 0.1093g respectively.

3.4 Substrate preparation:

A slab of SS 316 L was cut into 1cm×1cm pieces having thickness of 2.5 mm through mini electric circular saw. The edges were smoothed by buffing wheel made of steel wires. For grinding sample was first mounted with Bakelite powder at 180°C for 45 mins using hot mounting press. Then it was grinded on grinding machine with different SiC emery paper.

P120 to P600 grit emery paper were used for grinding. After grinding on each paper sample was rotated 90 degrees to avoid deepening of scratches. The sample was then demounted by breaking Bakelite mold through bolt and wire cutter. This demounted sample was then placed in a glass beaker (100ml) and acetone was added in the beaker until sample get submerged in acetone. Beaker was placed in ultrasonic bath at room temperature for 20mins of sonication. Sample was sonicated in ethanol and DI water respectively through same technique. Sonicated sample was then dried in drying oven and thus substrate is ready for coating.

3.5 Coating on Stainless Steel 316 L:

For coating 1 gram of hydroxyapatite powder was added in 500µl (DMF, Honeywell) and kept for stirring overnight on a hot plate. The prepared substrate was placed on spin coater, 20µl of hydroxyapatite solution was dropped using micropipette. The spin coater was set to 2000 rpm for 3mins. This coated substrate was placed in drying oven at 150°C for 10 mins. This process was repeated thrice. DMF and hydroxyapatite solution was continuously stirred during coating to avoid settling down of particles. This same procedure was followed for coating M1 and M2.

3.6 Characterization:

The pure HAp, substituted hydroxyapatite powder and coating were subjected to various characterization techniques to confirm the formation of the necessary product as outlined below.

3.6.1 X-Ray Diffraction:

X-Rays are part of the electromagnetic spectrum. They are produced when high energy electrons are bombarded on any heavy metal. Mosely's law tells us that each element

has its signature x-rays ($K\alpha$) which depend on the mass number of each element. X-rays have smaller wavelengths than visible light and can penetrate inside crystallographic structures.

$$\lambda/2 \leq D$$

Their wavelength is also comparable with interatomic distances (D) which makes it suitable for attaining crystallographic information of any material. Diffraction is the main technique through which we identify crystal structure.

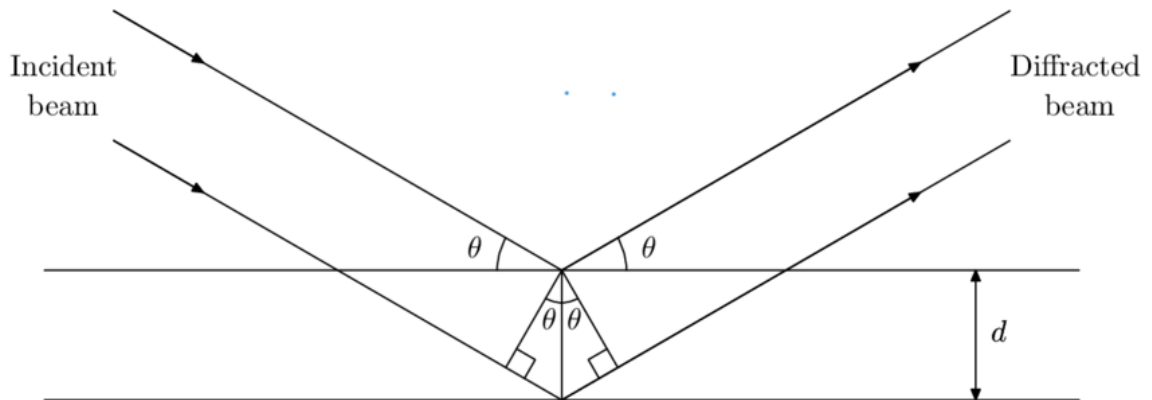


Figure 15 Bragg's law schematic illustration [71].

As illustrated in Figure 15 when two parallel beams are diffracted through a single slit then path difference obtained is $d \sin \theta$, but when parallel beams are incident on slit through an angle then path difference becomes $2d \sin \theta$ [72]. In crystal structure interatomic distances act as diffraction slits and we already know that this path difference is equal to λ or integral multiple of λ which is known as Bragg's law:

$$2d \sin \theta = n\lambda$$

In the X-ray spectrometer, an X-ray tube emits X-rays towards a sample that is positioned on a sample holder located at the center of the tube and the detector. The incidence of X-rays on the sample stimulates the electrons of the sample, which subsequently return to their original state by re-emitting unique X-rays for each material.

The emitted X-rays are captured by a detector situated on the opposite side of the sample holder. Both the X-ray tube and the detector are mobile.

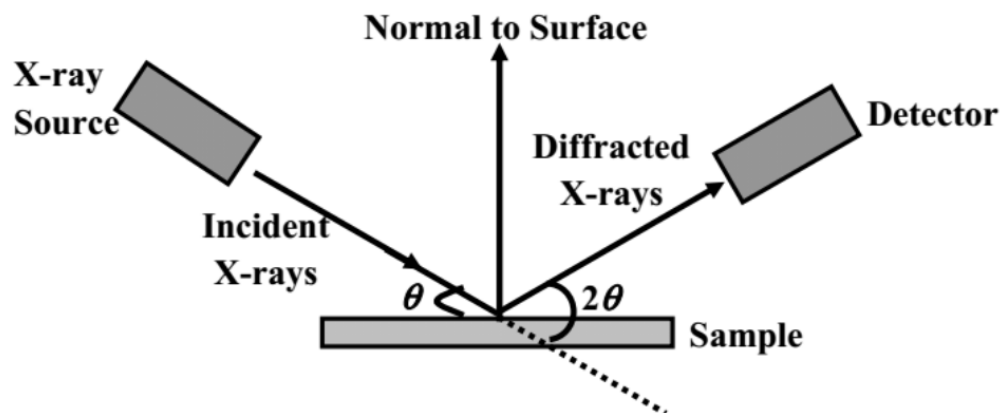


Figure 16 X Ray spectrometer schematic [72].

The schematic of X Ray spectrometer [73] is illustrated in Figure 16. Data collected by detector is presented in the form of a graph. The aim of conducting X-ray diffraction (XRD) analysis is to ascertain the crystallographic configuration of materials, recognize distinct phases, measure their relative abundance, and gauge lattice parameters and strains. This technique is extensively employed in multiple scientific domains to scrutinize the properties of materials and confirm the quality of products in industrial applications. The sample was dried at 100°C for 1 hour before analysis.

3.6.2 Fourier Transform Infrared Spectroscopy (Powder):

FTIR stands for Fourier transform infrared spectroscopy. It is used to analyze molecular structure and composition of molecular mixtures. It uses modulated mid infrared energy to interrogate a sample. Infrared light is absorbed at specific frequencies which are directly related to the atom-to-atom vibrational bond energies in the molecule when both energies of mid infrared light and vibrational bond energies becomes equivalent then bond can absorb infra-red energy. Different bonds in molecules vibrate at different energies and absorb infra-red radiation according to their own energy. The frequency and intensity of these absorbed wavelengths contribute to the overall spectrum creating characteristic fingerprint of the molecule. Since FTIR observes functional groups of

molecules it is an ideal technique to measure the making and breaking of chemical bonds.

FTIR follows beer lambert law i.e.

$$A=abc$$

Where 'a' is molar absorptivity, path length is 'b' both of which are constants and 'c' is concentration so absorbance 'A' that a vibrational frequency for a specific is directly proportional to the concentration of specific bond [74].

FTIR spectrometer has following main components:

- Source
- Collimator
- Interferometer
- Sample
- Detector

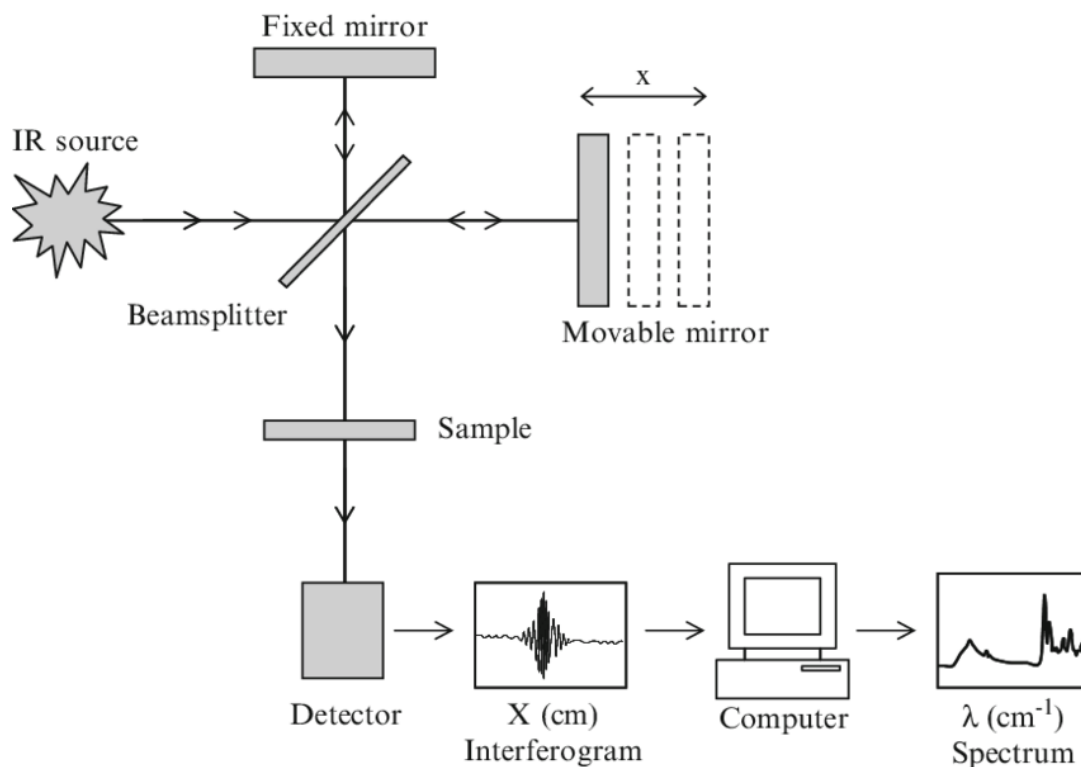


Figure 17 FTIR instrumentation [74].

Different types of sources such as GLOBAR source, NERNST source etc. Tungsten halogen lamp can be used for near infrared region whereas mercury lamp is used for far infrared region. Electromagnetic radiation from 4000 to 400 cm^{-1} is needed.

An important component in FTIR is Michelson interferometer this acts like a monochromator Figure 17 illustrates FTIR instrumentation [75]. It has 3 basic components one is a beam splitter which splits incident radiation into two equivalent radiations. It is made up of germanium coated with KBr, second it has He-Ne laser beam which is responsible for the accuracy. Third component is two mirrors one is fixed while other is movable radiation comes from source after passing through collimator then it strikes beam splitter which splits it in two components one component of IR radiation is directed towards fixed mirror and other component travels to moveable mirror. Radiation through both mirrors falls back on beam splitter which reflects radiation towards sample. If the distance between fixed and movable mirror is same (zero path difference) then constructive interference happens and if distance is not equal (optical path difference) destructive interference happens. Through this mechanism a variety of wavelengths are transmitted to a sample which absorbs radiation which is same as their bond energy and transmits remaining radiation to the detector. An interferogram is recorded by a detector which records absorbance w.r.t time in the form of graph. Fourier transform equation is applied on this data to convert intensity vs time graph into intensity vs frequency graph. This whole calculation is done automatically through pre-installed software. The primary objective of Fourier Transform Infrared (FTIR) spectroscopy is to ascertain and scrutinize the chemical composition of a given sample through the quantification of infrared radiation absorption. This analytical method offers valuable insights into the functional groups, molecular vibrations, and chemical bonds present in a diverse array of materials, thereby facilitating the identification of materials, quality control, and research in various domains such as chemistry, pharmaceuticals, polymers, and environmental science. For sample preparation powdered sample was first converted into a round disk through die in which we add potassium bromide (KBr) to cover the inner cavity of die properly then little amount of sample is sprinkled on KBr powder then this die is subjected to high pressure through hydraulic press which converts powdered KBr and sample into a small round disc.

3.6.3 Scanning Electron Microscope:

Scanning electron microscope is a type of electron microscopy. Electron beam is used to illuminate the specimen and create magnified images. Magnification of SEM is as low as 20x to 50x to as high as one million. Resolution of SEM is between 0.5 and 4 nanometers. This microscope is attached to a computer which generates images obtained by microscope. SEM is used to observe the morphology of the sample. It consists of cathode, anode, electromagnetic lenses, detector, and raster scan generator. All these components are enclosed in a chamber which has two parts, the upper part is known as column and lower part is known as specimen chamber. The whole chamber is attached with a vacuum pump so that the surrounding environment cannot interact with our specimen, and we can obtain a clear image of specimen [76].

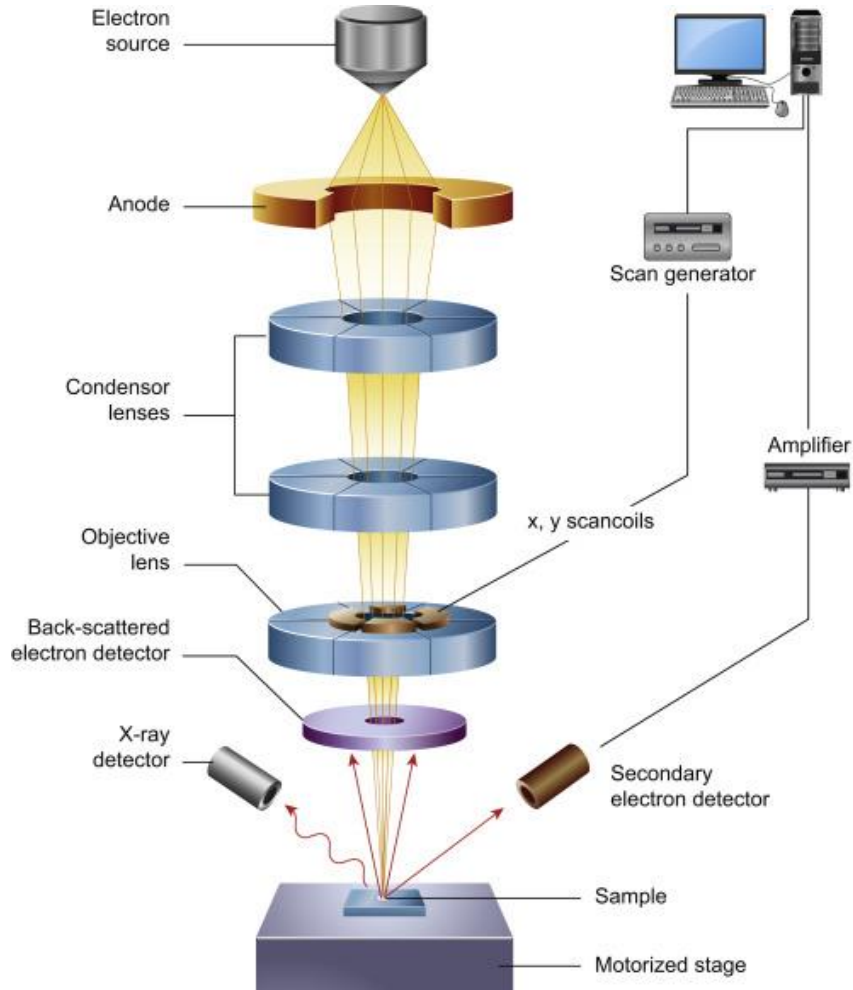


Figure 18 SEM Instrumentation [75].

V shaped tungsten wire is used as thermionic cathode which emits electrons. These electrons accelerate towards the anode because it bears positive charge. Then this electron beam is passed through electromagnetic lenses which makes it focused on specimen. This electron beam consists of primary electrons. After electromagnetic lenses we have electromagnetic deflector and raster scan generator which helps beam to deflect and scan whole specimen surface area. We have three types of detectors around the specimen: secondary electron detector, back scattered electron detector and x-ray detector. All of this is shown in Figure 18 . When electron beam falls on specimen then different types of emission takes place that are secondary electron, back scattered electrons, and characteristic x-rays of the specimen. Following Figure 19 represents this emission [77].

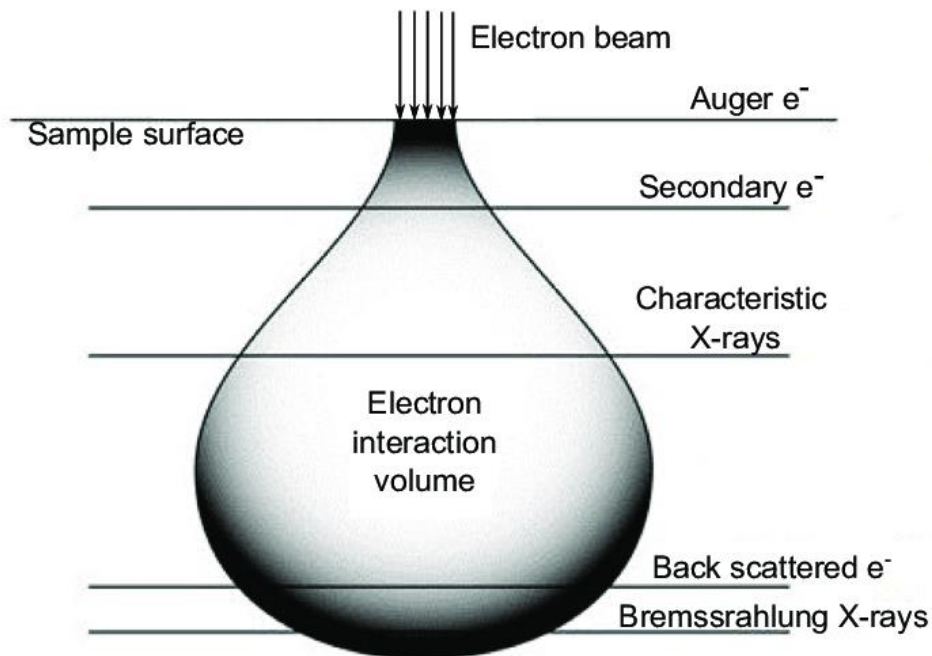


Figure 19 electron emission from sample in SEM [76].

The aim of utilizing SEM is to procure images of elevated resolution pertaining to the surface morphology of a specimen. This technique grants researchers the ability to perceive and scrutinize the microstructure, surface topography, and elemental composition of materials at an extremely minute scale, thus affording valuable insights into sundry fields. Sample preparation was conducted before placing it on specimen

stage of this microscope. Sample must be dried well and then coated with aluminum or gold particles for better conduction of electrons from tip of to sample.

3.6.4 Energy dispersive X-ray (EDX):

Energy dispersive x-ray is a technique used for elemental analysis of specimens. The primary objective of EDX is to conduct an elemental composition assessment of a given sample. It is commonly utilized in tandem with SEM to effectively discern and accurately quantify the elements contained within a material or its surface. EDX presents an array of informative data concerning the chemical composition, distribution of elements and impurities present in a sample, which renders it an influential tool in materials characterization. When a high energy beam of electrons falls on the sample it knocks out electrons from the inner shells of atoms. Electrons from outer shells then jump into the vacant space of inner shells emitting characteristic rays. These rays are known as x-rays, and these are specific for each element. Through observing these rays, we analyze the elements present in our sample.

3.6.5 Corrosion testing (Coated sample):

Gamry interface 1010E and Biological VSP potentiostat is used for this characterization. Three electrode cell configuration is used for corrosion testing. In which one is working electrode second is reference electrode and third electrode is known as counter electrode. Platinum wire was used as a counter electrode. Ag/AgCl was used as reference electrode and our sample was used as working electrode. The ringer solution was prepared to be used as electrolyte then the back of our sample was attached with a wire using epoxy. This sample was then dipped in ringer solution for at least 6 hours before testing.

3.6.5.1 Open circuit potential:

When a circuit or electrochemical cell is not linked to any load or has current flowing, it is said to have an open circuit potential (OCP), also referred to as an open circuit voltage (OCV). It is the potential difference between two electrodes or terminals of a system or device while it is not in use. The thermodynamic behavior of an electrochemical cell is frequently assessed in the context of electrochemistry using the open circuit potential. A potential difference between the electrodes results from the electrode reactions even when a cell is not linked to any external load. The equilibrium between the oxidation and reduction reactions occurring at the electrodes is reflected in this potential difference

[49]. During corrosion investigations, open circuit potential is frequently measured. Open circuit potential can change depending on elements like temperature, the makeup of the electrodes and the solution, as well as other external conditions.

3.6.5.2 Electrochemical Impedance Spectroscopy:

A potent electrochemical method used to investigate the electrical characteristics and behavior of electrochemical systems is electrochemical impedance spectroscopy (EIS). It entails perturbing the system with a tiny, sinusoidal signal and monitoring the current response that results over a range of frequencies. In EIS, a constant bias potential is overlaid with a tiny amplitude alternating current (AC) signal. The AC signal's frequency is varied widely, often between millihertz and megahertz, covering both low and high frequencies [49, 78]. Impedance consisting of both magnitude and phase is measured in the electrochemical system as complex quantity. The ratio of the voltage response to the applied current perturbation is known as the impedance. It is possible to deduce important details about the electrical characteristics and workings of the system by studying the impedance response at various frequencies[57]. EIS can provide data about many electrochemical phenomena such as corrosion.

3.6.5.3 Potentio-dynamic polarization:

An electrochemical method for examining the corrosion behavior of metallic materials is potentiodynamic polarization. It includes varying the applied voltage over a predetermined range while monitoring the current response of an electrochemical cell.

Three steps are involved in this process which are as follows:

1. Potentiostatic Equilibration: The first step entails maintaining the working electrode at a constant potential, typically the metal under investigation, to permit the development of a reliable electrochemical equilibrium. Before moving on to the next level, this stage makes sure the system enters a steady state.
2. Potential Sweep: During this phase, the working electrode's potential is constantly swept at a predetermined pace over a predetermined range. Depending on the desired analysis, the potential sweep can be carried out either in the anodic (positive potential) or cathodic (negative potential) direction.
3. Data collection: The current response that is produced because of the applied potential is measured and recorded during the potential sweep. A potentiodynamic

polarization curve, which illustrates the relationship between the applied potential and the resulting current density, is created using the data that was obtained. This curve offers important details regarding the corrosion behavior of the material under investigation, including its critical pitting potential, corrosion potential, and corrosion current [49, 79, 80].

Researchers can learn more about the corrosion resistance, susceptibility to localized corrosion (such pitting or crevice corrosion), and general electrochemical behavior of a material in various situations by analyzing the potentiodynamic polarization curve[57]. This knowledge is essential for designing and choosing materials for corrosion-sensitive applications, such as those found in the automotive, aerospace, and marine sectors.

3.6.6 Optical Profilometry:

Optical profilometry is a non-destructive, non-contact technique used for measuring surface roughness, profile and topography shape and form. It uses coherence scanning interferometry to generate desired results [81]. It has 80 μ m to 60mm field of view. Wave properties of light named phase and coherence for this technique were used. Interferometer is a basic component of profilometer. Single beam is emitted from the source split in the two paths by beam splitter (half silver mirror). Reference path length is fixed whereas test path length is variable. The test path length is scanned with both test path and reference path reflecting on the beam splitter. Recombined paths are measured by a detector [82]. An interference pattern is obtained on the detector due to the change in height of test path. Hence providing us with the information of surface roughness of sample.

3.6.7 Contact angle:

Contact angle is measured using a goniometer or optical tensiometer which consists of camera, sessile liquid dropping setup, stage for sample and computer with which camera is attached. The stage for sample and camera is inline and it can be moved through computer. A water drop is dropped on the sample surface which is then observed through camera young's equation is used to identify the contact angle and wettability of the sample [83].

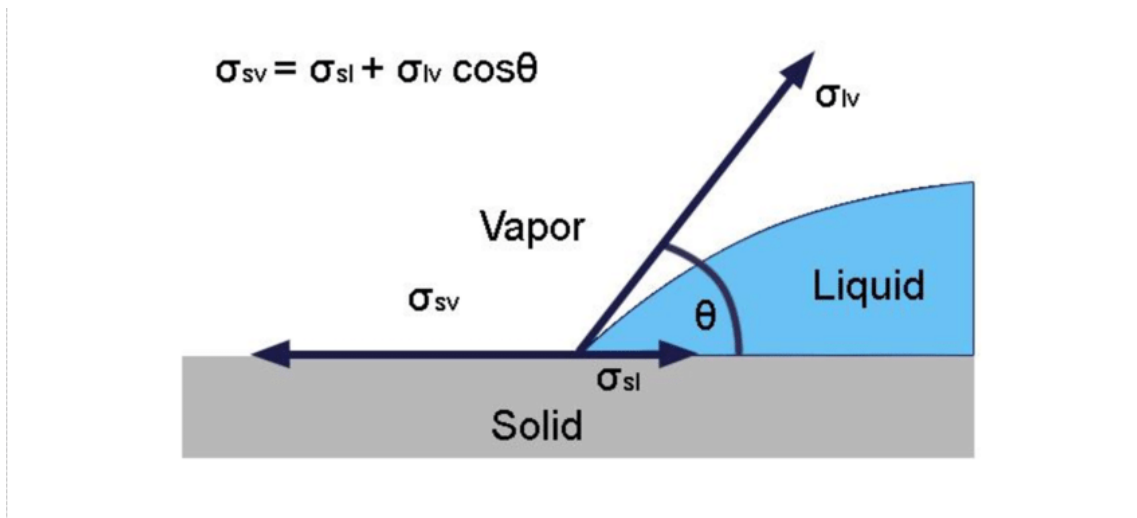


Figure 20 young's equation and contact angle representation [83].

Figure 20 illustrates method of calculating contact is angle [84]. Contact angle is an angle which is formed by the drop on sample at three phase boundaries where solid liquid and gas intersects. If the contact angle is less than 90° then the surface is hydrophilic, if it is greater than 90° then surface is hydrophobic.

3.6.8 Antibacterial testing:

Antibacterial susceptibility testing, also referred to as antimicrobial susceptibility testing or AST, is a laboratory protocol employed to evaluate the efficacy of antibiotics or other antimicrobial agents against bacterial strains that are obtained from clinical specimens. The primary objective of this testing is to gauge the susceptibility or resistance of bacteria to specific antibiotics, thereby helping clinicians in selecting the most appropriate and efficacious treatment for bacterial infections. The testing entails exposing the bacterial isolate to varied antibiotics at predetermined concentrations, and subsequently observing the bacterial growth response. The two most utilized methods for antibacterial susceptibility testing are:

The Kirby-Bauer Method: Also known as the Disc Diffusion Method in which the determination of bacteria susceptibility to antibiotics or antimicrobial agents is commonly accomplished by means of a widely employed test. This test serves the purpose of evaluating the effectiveness of specific antibiotics against bacterial strains, which have been isolated from clinical specimens [51, 58]. The test procedure comprises several steps:

1. **Bacterial Isolation and Inoculum Preparation:** This initial stage involves the isolation of bacteria from the patient's sample, for example, urine, blood or wound swab. The isolated bacterial colonies are subsequently cultured in nutrient broth to generate a standardized bacterial suspension, the inoculum. In order to ensure consistent and comparable results, the inoculum's turbidity is adjusted to match that of a 0.5 McFarland standard.
2. A sterile Mueller-Hinton agar plate is utilized as the growth medium for the preparation of Mueller-Hinton agar plates. The inoculum is uniformly spread across the surface of the agar with the aid of a sterile cotton swab.
3. Filter paper discs containing specific antibiotics are placed on the surface of the agar. These antibiotics are commercially available and are present in known concentrations on each disc.
4. Incubation of the inoculated agar plate with the antibiotic discs occurs at an appropriate temperature and duration, typically at 35-37°C for 16-18 hours.
5. Following incubation, the plates are analyzed for the presence of a clear zone around the antibiotic disc, indicating the effectiveness of the antibiotic against the bacterial strain. This zone, known as the "zone of inhibition", is measured in millimeters using a ruler or caliper.
6. The interpretation process involves comparing the diameter of the zone of inhibition with standardized interpretive charts, such as those provided by the Clinical and Laboratory Standards Institute (CLSI) or the European Committee on Antimicrobial Susceptibility Testing (EUCAST). This chart classifies the bacterial isolate as either susceptible, intermediate, or resistant to the tested antibiotic based on the zone size [56, 59].

The disc diffusion method is a simple, reliable, and cost-effective approach for determining bacterial susceptibility to antibiotics. Its implementation assists clinicians in selecting the most appropriate and effective antibiotic treatment for bacterial infections, thus contributing to better patient outcomes and the appropriate use of antibiotics to combat antibiotic resistance.

On the other hand, the Broth Dilution Method involves the preparation of serial dilutions of antibiotics within a liquid growth medium that contains the bacterial isolate. The

tubes or wells with varying antibiotic concentrations are then incubated, and the lowest concentration of the antibiotic that prevents visible bacterial growth is recorded. This minimal inhibitory concentration (MIC) value serves as a quantitative measure of the antibiotic's effectiveness against the specific bacterial strain.

The reporting of antibacterial susceptibility testing outcomes to healthcare providers aids in the selection of the most suitable antibiotic therapy for patients. It is imperative to customize the treatment to the specific patient, considering variables such as infection type, medical history, and regional patterns of antibiotic resistance, to guarantee optimal treatment results and deter antibiotic resistance development.

Chapter: 4

4 Results & Discussions

4.1 X- Ray Diffraction Analysis:

X-ray analysis of hydroxyapatite powder, modified hydroxyapatite powder with both ratios M1 and M2 have been conducted. In Figure 21 hydroxyapatite is represented in black, M1 is represented in red and M2 is represented in blue color. Graph shows sharp peaks with high intensity which indicates well crystallized material. The prominent planes are (0 0 2), (2 1 1), (1 1 2), (3 0 0), (2 0 2), (3 1 0), (2 2 2), (2 1 3) at 25.7°, 31.7°, 32.1°, 32.9°, 34°, 39.8°, 46.7° & 49.5° angle respectively which corresponds to characteristic peaks of hydroxyapatite in literature and JCPDS file no. 9-0432 [78].

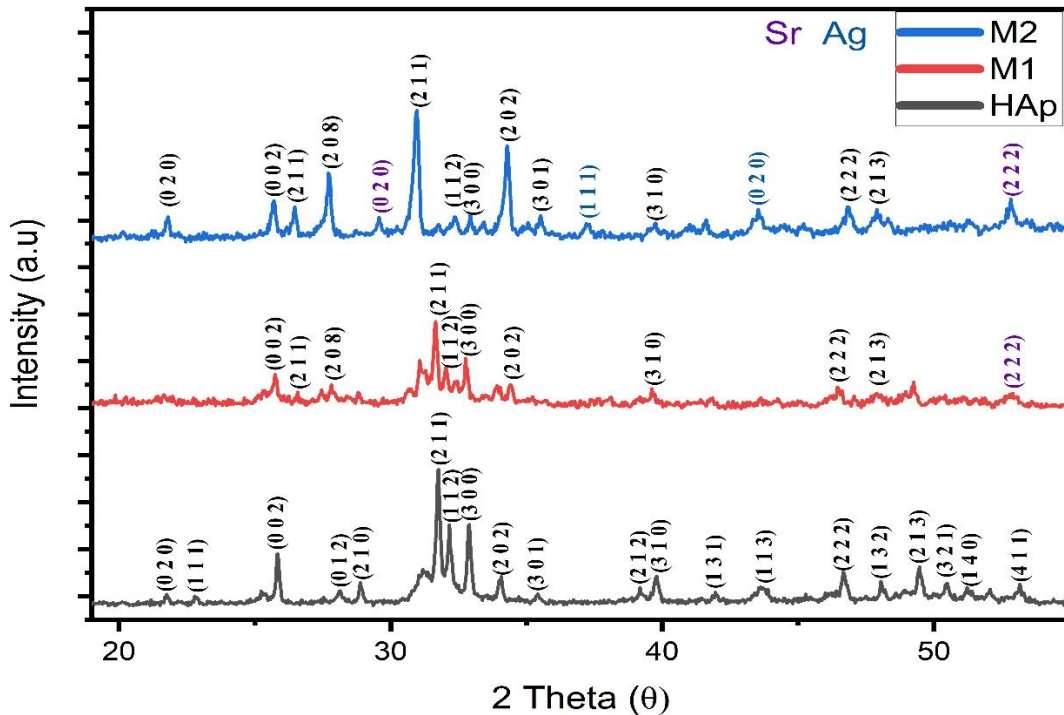


Figure 21 XRD of HA, M1 & M2

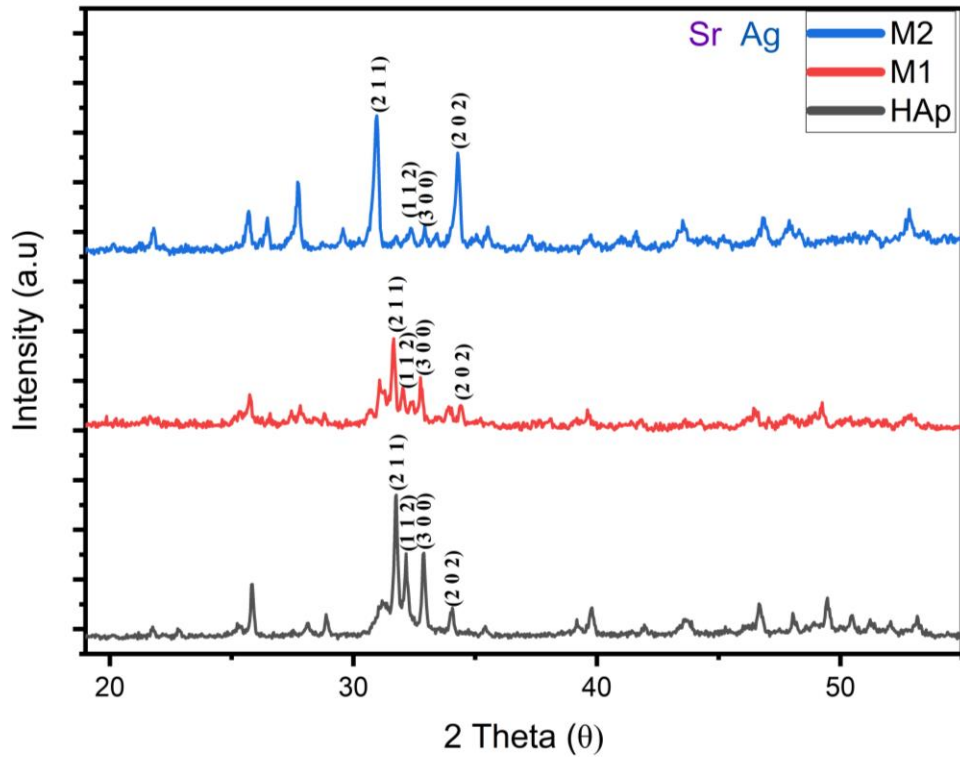


Figure 22 major peaks of HAp, M1 & M2

Modified hydroxyapatite M1 ($\text{Ag} > \text{Mg}$) graph due to substitution of Sr^{2+} , Mg^{2+} and Ag^+ in HA lattice peaks from 30° to 32° are a bit broadened, shifted at lower angle and less intense while overall all the peaks indicate HAp as sole crystalline phase. This indicates the substitution of other ions in place of Ca^{2+} . As reported in literature substitution of strontium, magnesium causes peak broadening [30, 85] and high concentration of silver makes lattice more crystalline which hindered shift in 2Θ [52]. Figure 22 shows the XRD pattern of HAp, M1 & M2 in which only major peaks are labeled. In modified hydroxyapatite M2 ($\text{Ag} < \text{Mg}$) graph shows prominent peak shift from theta 31.7 to 30.9 which is shown in Figure 23 below, this is due to less concentration of Ag and specific concentration of Sr. Similar result was also reported in literature [58]. These attributes in graphs confirm the substitution of Sr^{2+} , Mg^{2+} and Ag^+ substitution in HA lattice.

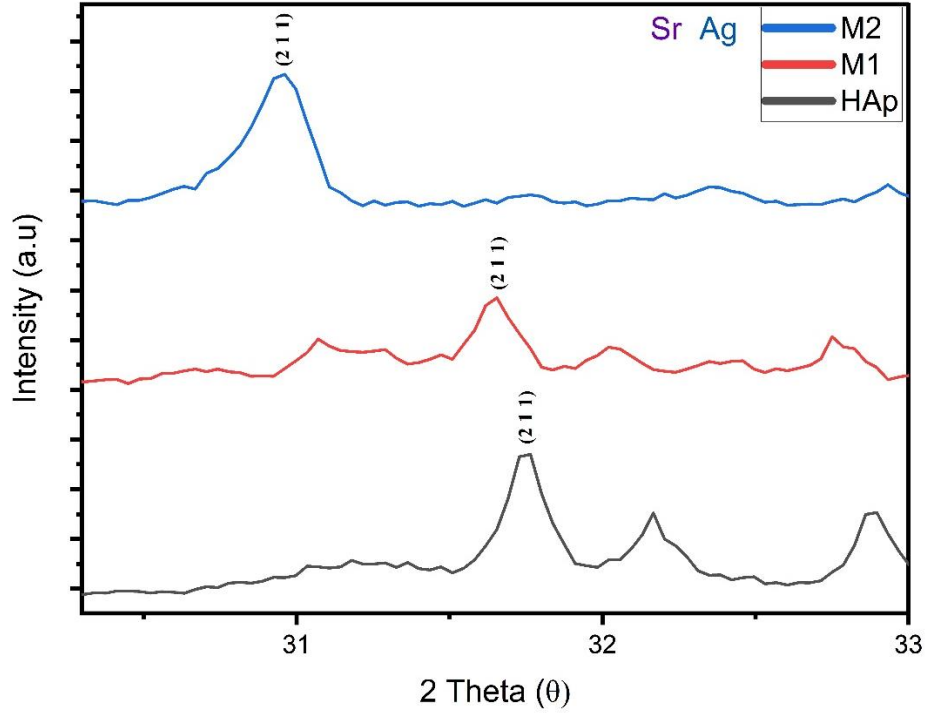


Figure 23 Zoomed in XRD to show peak shift.

Figure 24 (a) shows XRD graph of coated SS 316 L with HAp and Figure 24 (b) shows XRD graph of M1 & M2. In both graphs characteristic peak of HAp at (2 1 1) plane can be observed in HAp graph this peak is at 31.7° while in M1 & M2 graph peak shift of (2 1 1) plane can be observed from 31.7° to 30.9° as discussed above. A characteristic plane (1 1 1) at 44.3° of SS 316L is also shown.

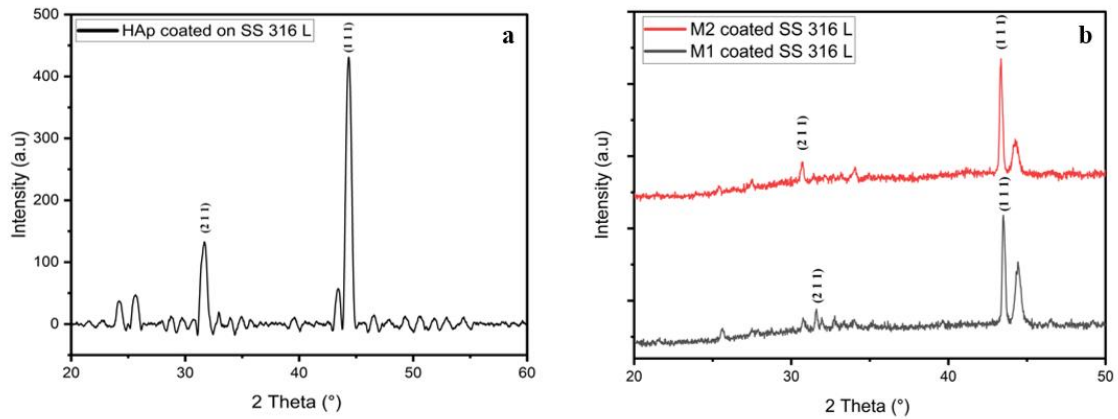


Figure 24 XRD of (a) HAp coated SS & (b) Modified HA coated SS.

4.2 FT-IR Analysis:

FT-IR analysis was conducted for hydroxyapatite and modified hydroxyapatite M1 and M2 powder. In Figure 25 HAp spectra show characteristic $-OH$, CO_3^{2-} , PO_4^{3-} and HPO_4^{2-} groups. $-OH$, shows absorption spectra from 3400 cm^{-1} to 3600 cm^{-1} with specific peak at 3570 cm^{-1} . CO_3^{2-} shows peaks between 1400 cm^{-1} to 1650 cm^{-1} [86]. PO_4^{3-} shows absorption spectra from 560 cm^{-1} to 650 cm^{-1} and 1040 cm^{-1} shows stretching vibrations.

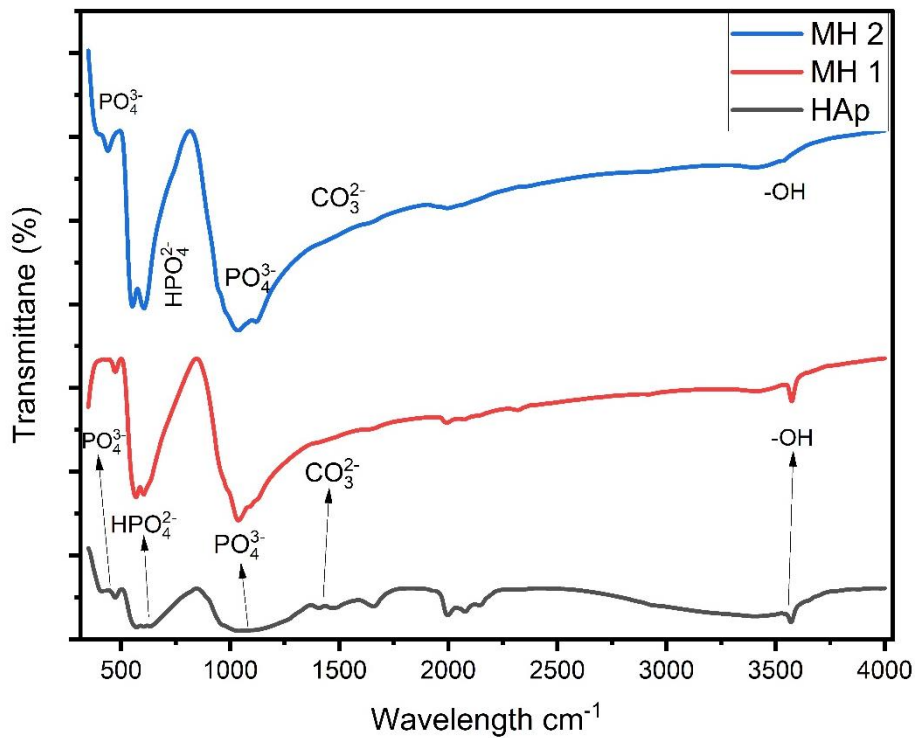


Figure 25 FTIR of HA, M1 & M2

M1 and M2 overall show the same behavior with slight broadening of peaks of -OH group and CO_3^{2-} group which confirms the substitution of Ag^+ , Sr^{2+} , Mg^{2+} ions in hydroxyapatite lattice as individual substitution peaks of strontium, silver & magnesium do not appear in FT-IR spectra. [56, 58].

4.3 Scanning Electron Microscopic Analysis:

SEM analysis of both powder and coated sample had been conducted. Figure 26 SEM images of (a) HAp, (b) M2. Figure 26 (a) shows image of HA powder in which agglomerated particles can be observed [58, 87], and in Figure 26 (b) SEM image of M2 shows flake like particles. In cross-section image of coated sample, $100 \pm 2 \mu\text{m}$ thickness is observed. The coating is dense and uniform. SEM images of coated sample is shown in Figure 27.

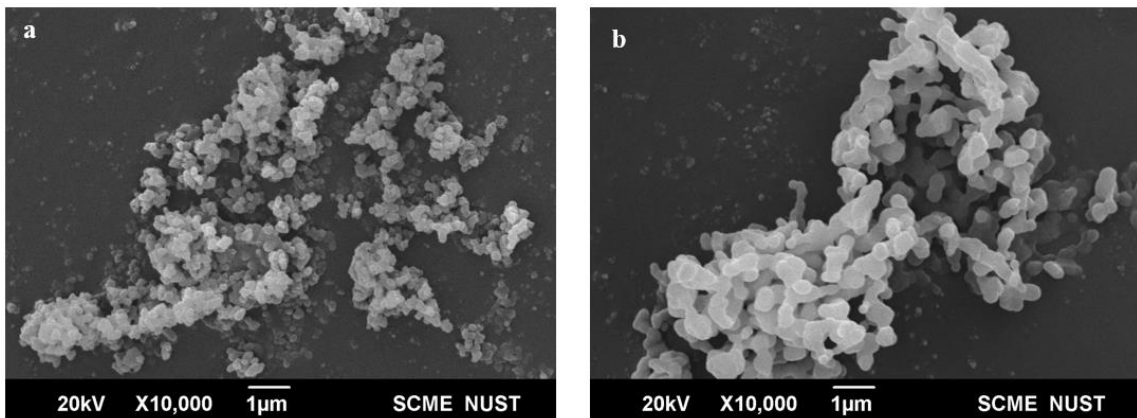


Figure 26 SEM images of (a) HAp, (b) M2

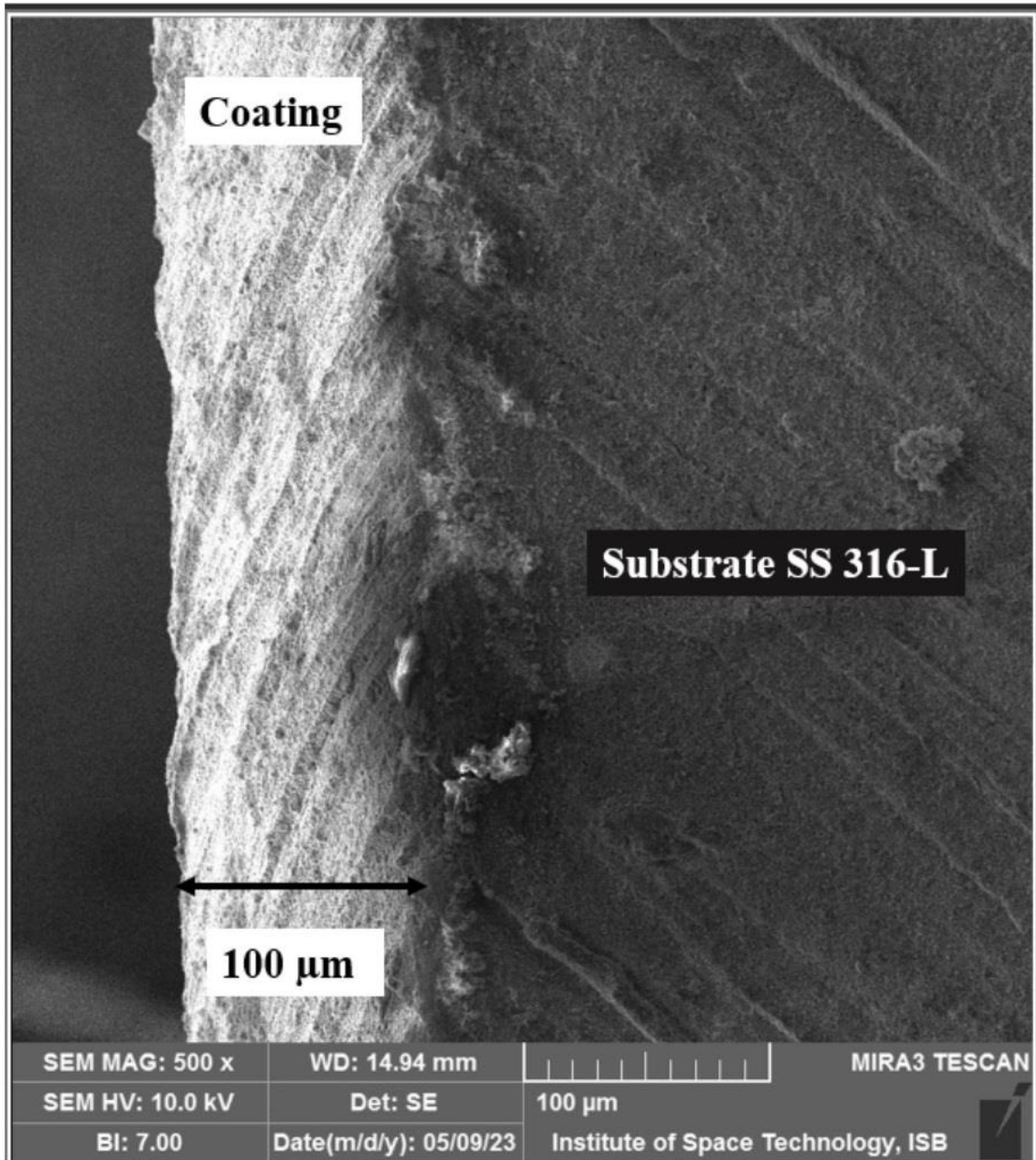


Figure 27 SEM image of cross-section of coated SS 316 L with M2

4.4 Corrosion Testing:

Corrosion testing was conducted to obtain the OCP, EIS, and Potentiodynamic polarization results. OCP, which determines the corrosion potential of the working

electrode in the absence of external potential to the electrochemical cell, was obtained after the working electrode was submerged in the ringer solution for six hours and test was run for 3600 secs each. The results indicate that the OCP of the bare SS 316L sample was -0.229mV, whereas the M2-coated SS 316L exhibited a potential of 0.097mV, demonstrating significant corrosion resistance. Table 2 tells us about the improved EIS and Potentiodynamic polarization measurements.

Table 2 Potentio-dynamic polarization results

Sample	Rp value	E corr	I corr	Corrosion Rate
SS 316L	$71.92 \times 10^3 \Omega \text{ cm}^2$	-558 mV	16.60 μA	6.846 Mpy
M2	$174.7 \times 10^3 \Omega \text{ cm}^2$	-454 mV	692 μA	284.9 $\times 10$ Mpy

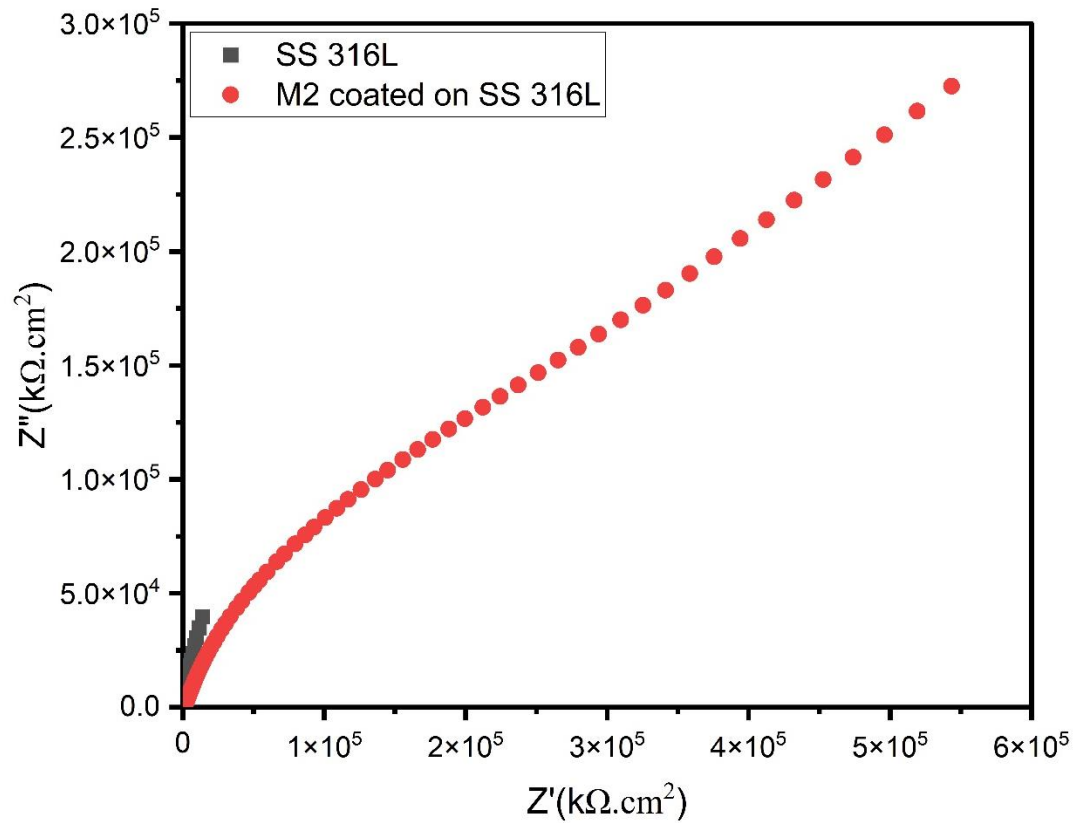


Figure 28 Nyquist plot of SS 316L & M2

The Nyquist plot obtained from EIS testing shows significantly increased resistance value after coating which is also demonstrated through graph in Figure 28. Through Potentiodynamic polarization curve values of E corr, I corr & corrosion rate was

determined. These value shows that coating of M2 on SS 316L was effective and caused a maximum shift in the noble direction when compared to the values obtained from bare SS 316L sample. Figure 29 shows shift in polarization curve.

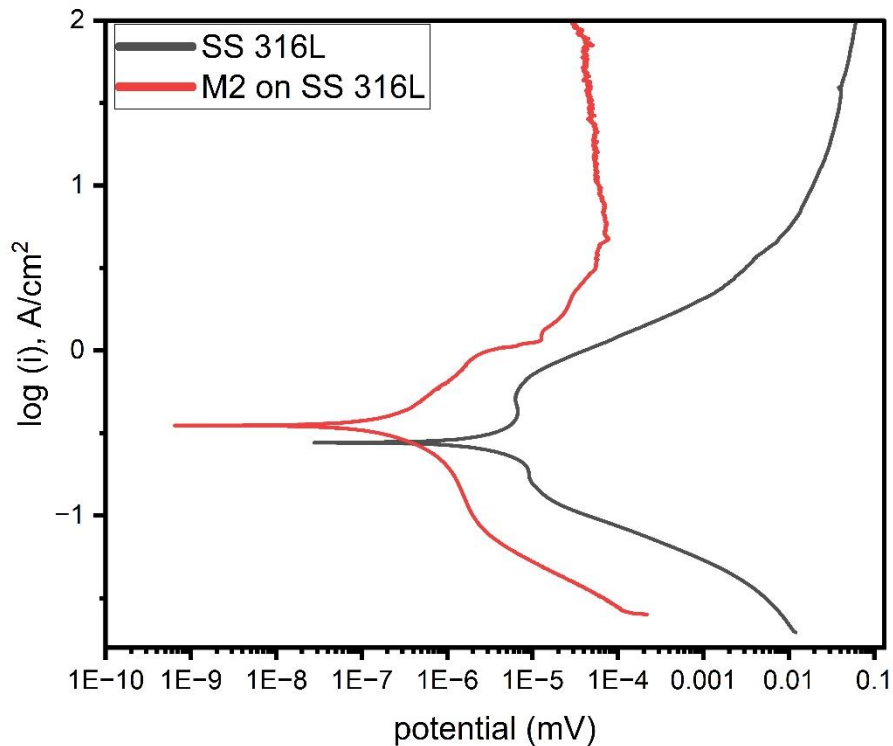


Figure 29 Potentiodynamic polarization curves of SS 316L & M2

4.5 Anti-bacterial Testing:

Silver, along with strontium and magnesium, was incorporated into hydroxyapatite due to its antibacterial properties. This substitution was necessary as the administration of antibiotics may not be effective on the implant surface. The release of silver ions was analyzed using the agar disc diffusion test [56, 58, 64], as depicted in Figure 30. In this test, hydroxyapatite substituted with silver, magnesium, and strontium produced an inhibition zone around the disc, whereas hydroxyapatite alone did not exhibit any inhibition zone. To evaluate the efficacy of the synthesized HAp, M1, M2, and control, *E.coli* bacteria was cultured on a Petri dish onto which the discs were placed individually. Solution of each powder was prepared in distilled water with 100% concentration.

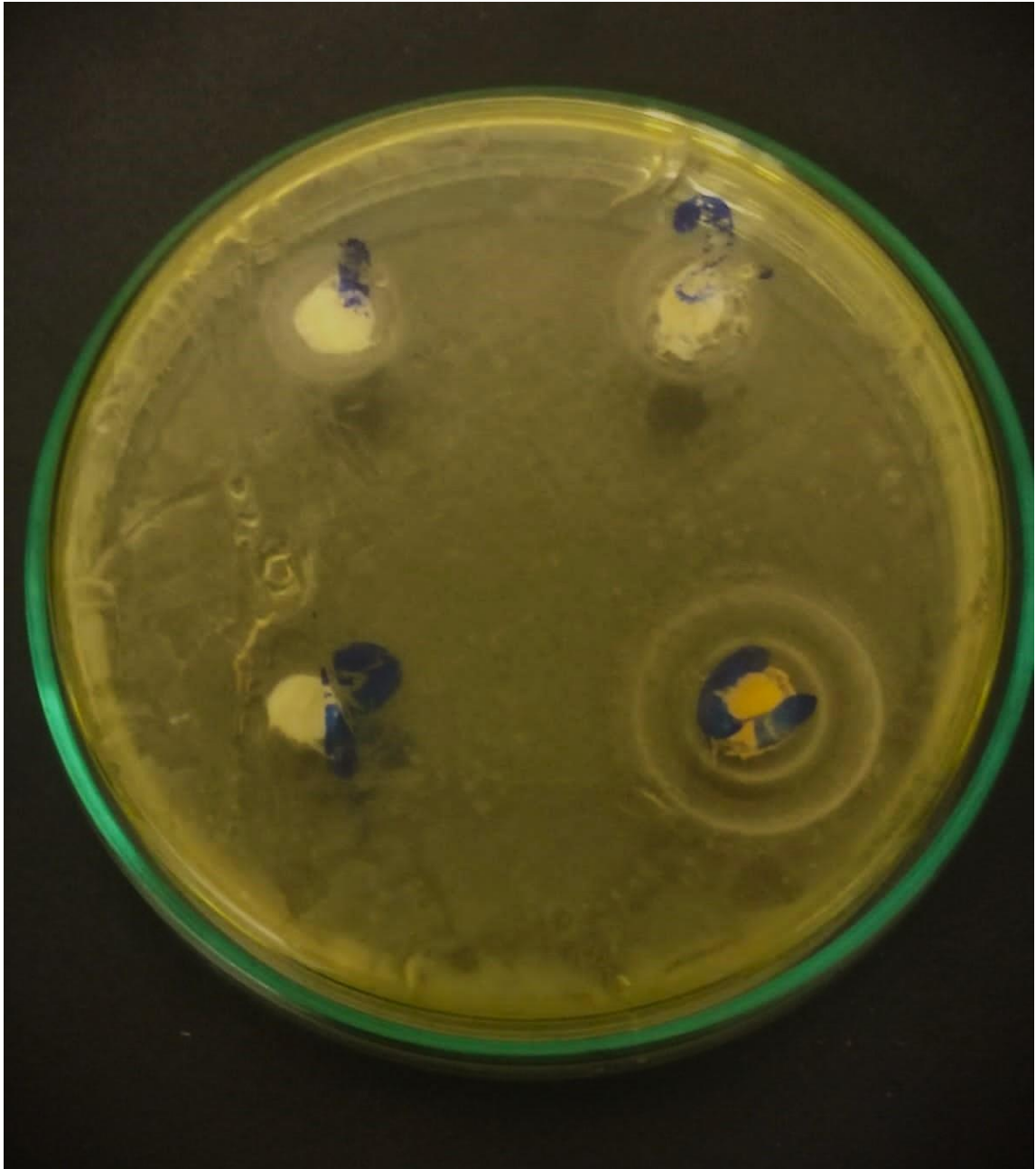


Figure 30 Agar disc diffusion test.

In the depicted figure, four discs were arranged and labeled as 1, 2, P, and C, signifying M1, M2, HAp, and control, respectively. The disc immersed by M1 solution exhibited an inhibition zone of roughly 1.4 cm in diameter. Similarly, an inhibition zone with a diameter of 1.6 cm, slightly larger than M1, was observed around the disc immersed with M2. The control disc, labeled as 'C' having Cyprofloxin solution, an efficacious antibiotic against *E.coli* bacteria, displayed a prominent inhibition zone of 2.4 cm in

diameter, demonstrating its effectiveness against *E.coli* bacteria. In contrast, Hydroxyapatite displayed no inhibition zone, thus indicating zero antibacterial activity. The findings of this study suggest that the antimicrobial activity observed is attributable to the silver ions that are released from the discs [51, 59, 88, 89]. Silver ions possess a high level of reactivity towards bacteria owing to their ability to penetrate the cell membrane of bacteria. This, in turn, triggers the disruption of the cell membranes of bacteria, thereby increasing their permeability and leading to the leakage of essential cellular components. Furthermore, silver ions can interfere with bacterial enzymes, DNA replication, and protein synthesis, ultimately resulting in bacterial death. Additionally, silver ions can stimulate the production of reactive oxygen species (ROS) within bacterial cells. ROS are known to be highly reactive molecules that can cause damage to cellular components such as DNA, proteins, and lipids. The accumulation of ROS can trigger oxidative stress, which can ultimately lead to bacterial cell death.

4.6 Optical Profilometry:

Optical profilometry is done to analyze the surface roughness of coated sample. Ra (surface roughness) of coated modified hydroxyapatite is $2.35 \pm 2 \mu\text{m}$. Surface roughness of SS 316 L (uncoated) is $0.15 \pm 2 \mu\text{m}$. The significance of surface roughness in implants lies in its ability to promote superior bone cell adhesion and growth, resulting in successful osseointegration. This is attributed to the increased surface area and microstructures that surface roughness offers, which facilitate the formation of a strong bone-implant interface. Moreover, surface roughness plays a pivotal role in the initial stability of the implant following surgical placement. The rough texture of the implant aids in gripping the surrounding bone more effectively during the early stages of healing, thereby reducing the risk of implant loosening or migration. Additionally, rough surfaces demonstrate a lower propensity for bacterial adhesion as compared to smooth surfaces. Given that orthopedic implants are highly susceptible to infections, minimizing bacterial colonization on the implant surface is crucial for reducing the risk of infection-related complications. This result indicates an increase in roughness which is ideal because of the above stated properties.

4.7 Contact Angle:

Contact angle is calculated to analyze nature of surface if it has angle $>90^\circ$ surface is consider hydrophobic while if angle is $< 90^\circ$ surface is considered hydrophilic. Shape of drop is shown in Figure 31 where (a) shows drop on M2 coated SS 316 L while (b) is bare surface of SS 316 L which is grinded at P600 emery paper and then ultrasonicated with acetone, ethanol, and DI Water respectively. We calculated uncoated SS 316 L sample which is $46.3^\circ \pm 6^\circ$ while contact angle of M2 coating on SS 316 L is $81^\circ \pm 1^\circ$. The phenomenon of wettability on the surface of an implant holds the potential to significantly impact the interface between the implant and the contiguous bone tissues during the process of osteointegration. The presence of a suitably angled contact on the surface of the implant has the capacity to catalyze cellular adhesion and augment bone growth around the implant, thereby elevating its stability and long-term efficacy. The following results indicate that our sample surface is hydrophilic and favorable for our application.

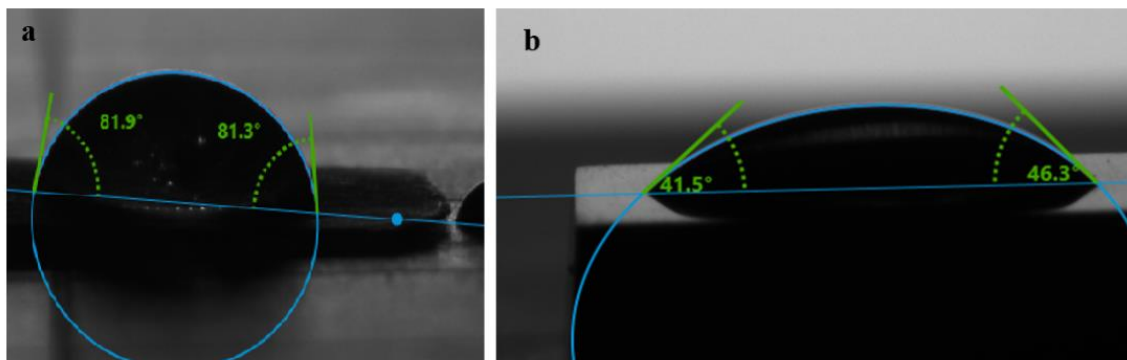


Figure 31 (a)M2 coated SS (b) bare SS surface.

4.8 Conclusion:

The process of wet precipitation was utilized to effectively synthesize Hydroxyapatite and modified Hydroxyapatite powder. These synthesized materials were then subjected to characterization via XRD, FT-IR and SEM, which revealed the presence of strontium, magnesium, and silver ions, as previously reported in literature. Additionally, coating of Hydroxyapatite and modified Hydroxyapatite was achieved through spin coating at 4000 rpm. Following this, OCP, EIS and Potentiodynamic polarization studies were conducted for corrosion testing. The results of these tests indicated an increase in the R_p

value from $71.92 \times 10^3 \Omega \text{ cm}^2$ to $174.7 \times 10^3 \Omega \text{ cm}^2$, along with a decrease in corrosion rate from 6.846 Mpy to 284.9×10^{-3} Mpy. Images of the coating's cross-section, as obtained via SEM, demonstrated a dense and uniform coating that was approximately $100 \pm 2 \mu\text{m}$ thick. Furthermore, the profilometer results showed that M2 coated SS 316L samples had an increased surface roughness, which is conducive to bone growth. Anti-bacterial activity was tested through agar disc diffusion method which shows inhibition zone having diameter 1.4 cm of M1 solution and 1.6 cm of M2 solution while HAp showed no inhibition zone.

References

- [1] Weinstein, A., et al., *Orthopedic implants—a clinical and metallurgical analysis*. (1973). **7**(3): p. 297-325.
- [2] Jin, W. and P.K.J.E.o.b.e. Chu, *Orthopedic implants*. (2019). **1**: p. 3.
- [3] Force, G.H.T. *Definition of the Terms ‘Medical Device’ and ‘In Vitro Diagnostic (IVD) Medical Device’*. May 16th, (2012).
- [4] D., A. *exactly what is medical device*. (2020) [cited (2023) 19 june]; Available from: <https://impactanalytical.wordpress.com/2020/03/03/exactly-what-is-a-medical-device/>.
- [5] Lee, J. and N.N.t. Kotov, *Thermometer design at the nanoscale*. (2007). **2**(1): p. 48-51.
- [6] Burkhard, S., et al., *On the evolution of the cardiac pacemaker*. (2017). **4**(2): p. 4.
- [7] Ledet, E.H., et al., *Smart implants in orthopedic surgery, improving patient outcomes: a review*. (2018): p. 41-51.
- [8] Enderle, J. and J. Bronzino, *Introduction to biomedical engineering*. (2012): Academic press.
- [9] Park, C.W., et al., *Reconstruction of a severely crushed leg with interpositional vessel grafts and latissimus dorsi flap*. (2012). **39**(04): p. 417-421.
- [10] Ratner, B.D., et al., *Biomaterials science: an introduction to materials in medicine*. (2004): Elsevier.
- [11] Hermawan, H., D. Ramdan, and J.R.J.B.e.-f.t.t.a. Djuansjah, *Metals for biomedical applications*. (2011). **1**: p. 411-430.
- [12] Pellatt, R., et al., *Is buddy taping as effective as plaster immobilization for adults with an uncomplicated neck of fifth metacarpal fracture? A randomized controlled trial*. (2019). **74**(1): p. 88-97.

- [13] Burny, F., et al., *Concept, design and fabrication of smart orthopedic implants*. (2000). **22**(7): p. 469-479.
- [14] Mattei, L., et al., *Lubrication and wear modelling of artificial hip joints: A review*. (2011). **44**(5): p. 532-549.
- [15] Cooke, F.W.J.C.O. and R. Research, *Ceramics in orthopedic surgery*. (1992). **276**: p. 135-146.
- [16] Agrawal, K., et al., *Synthesis and characterization of hydroxyapatite powder by sol-gel method for biomedical application*. (2011). **10**(8): p. 727-734.
- [17] Hamadouche, M., L.J.T.J.o.B. Sedel, and J.S.B. volume, *Ceramics in orthopaedics*. (2000). **82**(8): p. 1095-1099.
- [18] Lopez-Esteban, S., et al., *Bioactive glass coatings for orthopedic metallic implants*. (2003). **23**(15): p. 2921-2930.
- [19] Balasundaram, G. and T.J.J.M.b. Webster, *An overview of nano-polymers for orthopedic applications*. (2007). **7**(5): p. 635-642.
- [20] Middleton, J.C. and A.J.J.B. Tipton, *Synthetic biodegradable polymers as orthopedic devices*. (2000). **21**(23): p. 2335-2346.
- [21] Lommen, J., et al., *Metallic Artifact Reduction in Midfacial CT Scans Using Patient-Specific Polymer Implants Enhances Image Quality*. (2023). **13**(2): p. 236.
- [22] Wong, W.-K., et al., *Polymer–Metal Composite Healthcare Materials: From Nano to Device Scale*. (2022). **6**(8): p. 218.
- [23] Piconi, C. and S.J.J.o.C.S. Sprio, *Oxide bioceramic composites in orthopedics and dentistry*. (2021). **5**(8): p. 206.
- [24] Nayak, A.K.J.I.J.o.C.R., *Hydroxyapatite synthesis methodologies: an overview*. (2010). **2**(2): p. 903-907.
- [25] Brunton, P., et al., *Treatment of early caries lesions using biomimetic self-assembling peptides—a clinical safety trial*. (2013). **215**(4): p. E6-E6.
- [26] Wang, H., *Hydroxyapatite degradation and biocompatibility*. (2004): The Ohio State University.
- [27] Arcos, D. and M.J.J.o.M.C.B. Vallet-Regí, *Substituted hydroxyapatite coatings of bone implants*. (2020). **8**(9): p. 1781-1800.

- [28] Querido, W., A.L. Rossi, and M.J.M. Farina, *The effects of strontium on bone mineral: A review on current knowledge and microanalytical approaches*. (2016). **80**: p. 122-134.
- [29] Frasnelli, M., et al., *Synthesis and characterization of strontium-substituted hydroxyapatite nanoparticles for bone regeneration*. (2017). **71**: p. 653-662.
- [30] Tampieri, A., et al. *Magnesium doped hydroxyapatite: synthesis and characterization*. in *Key Engineering Materials*. (2004). Trans Tech Publ.
- [31] Zhang, J., et al., *Dual function of magnesium in bone biomineralization*. (2019). **8**(21): p. 1901030.
- [32] Sygnatowicz, M., K. Keyshar, and A.J.J. Tiwari, *Antimicrobial properties of silver-doped hydroxyapatite nano-powders and thin films*. (2010). **62**: p. 65-70.
- [33] Godbole, N., et al., *A review on surface treatment of stainless steel orthopedic implants*. (2016). **36**(1): p. 190-4.
- [34] Gutierrez Martinez, M., et al., *Characterization of SiO₂-TiO₂ Coatings on 316L Stainless Steel Substrates*. (2018). **6**(1): p. 3-13.
- [35] Pellier, J., J. Geringer, and B.J.W. Forest, *Fretting-corrosion between 316L SS and PMMA: Influence of ionic strength, protein and electrochemical conditions on material wear. Application to orthopaedic implants*. (2011). **271**(9-10): p. 1563-1571.
- [36] Suchanek, W. and M.J.J.o.m.r. Yoshimura, *Processing and properties of hydroxyapatite-based biomaterials for use as hard tissue replacement implants*. (1998). **13**(1): p. 94-117.
- [37] Irfan, M. and M.J.B.L. Irfan, *Overview of hydroxyapatite; composition, structure, synthesis methods and its biomedical uses*. (2020). **6**(1): p. 17-22.
- [38] Lett, J.A., K. Ravichandran, and M.J.J.C.P.R. Sundareswari, *The study on the synthetic methodologies for manoeuvring the morphology crystallinity and particle size of hydroxyapatite*. (2015). **7**: p. 231-239.
- [39] Koutsopoulos, S.J.J.o.B.M.R.A.O.J.o.T.S.f.B., The Japanese Society for Biomaterials,, T.A.S.f. Biomaterials, and t.K.S.f. Biomaterials, *Synthesis and characterization of hydroxyapatite crystals: a review study on the analytical methods*. (2002). **62**(4): p. 600-612.

- [40] Cengiz, B., et al., *Synthesis and characterization of hydroxyapatite nanoparticles*. (2008). **322**(1-3): p. 29-33.
- [41] Padmanabhan, S.K., et al., *Sol-gel synthesis and characterization of hydroxyapatite nanorods*. (2009). **7**(6): p. 466-470.
- [42] Doğan, Ö. and M.J.L. Öner, *Biomimetic mineralization of hydroxyapatite crystals on the copolymers of vinylphosphonic acid and 4-vinylimidazole*. (2006). **22**(23): p. 9671-9675.
- [43] Earl, J., D. Wood, and S. Milne. *Hydrothermal synthesis of hydroxyapatite*. in *Journal of Physics: Conference Series*. (2006). IOP Publishing.
- [44] Zhang, Y.-y., et al., *Electrochemical deposition of hydroxyapatite coatings on titanium*. (2006). **16**(3): p. 633-637.
- [45] Zhitomirsky, I. and L.J.J.o.M.S.M.i.M. Gal-Or, *Electrophoretic deposition of hydroxyapatite*. (1997). **8**: p. 213-219.
- [46] Šupová, M.J.C.i., *Substituted hydroxyapatites for biomedical applications: A review*. (2015). **41**(8): p. 9203-9231.
- [47] Capuccini, C., et al., *Strontium-substituted hydroxyapatite coatings synthesized by pulsed-laser deposition: in vitro osteoblast and osteoclast response*. (2008). **4**(6): p. 1885-1893.
- [48] Hongthong, B., S.K. Hodak, and S.J.A.M.R. Tungasmita, *Synthesis and characterizations of strontium substituted hydroxyapatite thin films*. (2010). **93**: p. 231-234.
- [49] Gopi, D., et al., *Corrosion protection performance of porous strontium hydroxyapatite coating on polypyrrole coated 316L stainless steel*. (2013). **107**: p. 130-136.
- [50] Gopi, D., et al., *Enhanced corrosion resistance of strontium hydroxyapatite coating on electron beam treated surgical grade stainless steel*. (2013). **286**: p. 83-90.
- [51] Prodan, A.M., et al., *Silver-doped hydroxyapatite thin layers obtained by sol-gel spin coating procedure*. (2019). **10**(1): p. 14.
- [52] Sivaraj, D. and K.J.U.s. Vijayalakshmi, *Enhanced antibacterial and corrosion resistance properties of Ag substituted hydroxyapatite/functionalized multiwall*

- carbon nanotube nanocomposite coating on 316L stainless steel for biomedical application.* (2019). **59**: p. 104730.
- [53] Tampieri, A., et al., *Magnesium doped hydroxyapatite: synthesis and characterization.* (2004). **264**: p. 2051-2054.
- [54] Rezaei, A., et al., *Hydroxyapatite/hydroxyapatite-magnesium double-layer coatings as potential candidates for surface modification of 316 LVM stainless steel implants.* (2020). **46**(16): p. 25374-25381.
- [55] Sutha, S., et al., *Mg-doped hydroxyapatite/chitosan composite coated 316l stainless steel implants for biomedical applications.* (2015). **15**(6): p. 4178-4187.
- [56] Gopi, D., et al., *Synthesis and spectral characterization of silver/magnesium co-substituted hydroxyapatite for biomedical applications.* (2014). **127**: p. 286-291.
- [57] Gopi, D., et al., *Development of strontium and magnesium substituted porous hydroxyapatite/poly (3, 4-ethylenedioxythiophene) coating on surgical grade stainless steel and its bioactivity on osteoblast cells.* (2014). **114**: p. 234-240.
- [58] Geng, Z., et al., *Strontium incorporation to optimize the antibacterial and biological characteristics of silver-substituted hydroxyapatite coating.* (2016). **58**: p. 467-477.
- [59] Saleem, O., et al., *Fabrication and characterization of Ag–Sr-substituted hydroxyapatite/chitosan coatings deposited via electrophoretic deposition: A design of experiment study.* (2020). **5**(36): p. 22984-22992.
- [60] Govindaraj, D. and M. Rajan. *Coating of bio-mimetic minerals-substituted hydroxyapatite on surgical grade stainless steel 316L by electrophoretic deposition for hard tissue applications.* in *IOP conference series: materials science and engineering.* (2018). IOP Publishing.
- [61] Vo, T.H., et al., *Electrodeposition and characterization of hydroxyapatite coatings doped by Sr²⁺, Mg²⁺, Na⁺ and F⁻ on 316L stainless steel.* (2018). **9**(4): p. 045001.
- [62] Park, J. and R.S. Lakes, *Biomaterials: an introduction.* (2007): Springer Science & Business Media.
- [63] Xu, S., et al., *RF plasma sputtering deposition of hydroxyapatite bioceramics: synthesis, performance, and biocompatibility.* (2005). **2**(5): p. 373-390.

- [64] Ciobanu, C., et al., *Antimicrobial activity evaluation on silver doped hydroxyapatite/polydimethylsiloxane composite layer*. (2015). (2015).
- [65] Khandelwal, H., et al., *Characterization of hydroxyapatite coating by pulse laser deposition technique on stainless steel 316 L by varying laser energy*. (2013). **265**: p. 30-35.
- [66] Mavis, B. and A.C.J.J.o.t.A.C.S. Taş, *Dip coating of calcium hydroxyapatite on Ti-6Al-4V substrates*. (2000). **83**(4): p. 989-991.
- [67] Asri, R., et al., *A review of hydroxyapatite-based coating techniques: Sol-gel and electrochemical depositions on biocompatible metals*. (2016). **57**: p. 95-108.
- [68] Singh, S., et al., *Sol-gel derived hydroxyapatite coating on Mg-3Zn alloy for orthopedic application*. (2015). **67**: p. 702-712.
- [69] Sutha, S., et al., *In-vitro bioactivity, biocorrosion and antibacterial activity of silicon integrated hydroxyapatite/chitosan composite coating on 316 L stainless steel implants*. (2013). **33**(7): p. 4046-4054.
- [70] Sidane, D., et al., *Biocompatibility of sol-gel hydroxyapatite-titania composite and bilayer coatings*. (2017). **72**: p. 650-658.
- [71] Singh, V., et al., *Synthesis and characterization of carbon nanotubes doped hydroxyapatite nanoceramic for orthopedic applications*. (2018). **71**: p. 177-183.
- [72] Sochi, T.J.a.p.a., *High throughput software for powder diffraction and its application to heterogeneous catalysis*. (2010).
- [73] Anduaem, W.W., *GREEN SYNTHESIS OF CUO NANOPARTICLES FOR THE APPLICATION OF DYE SENSITIZED SOLAR CELL*. (2020).
- [74] Berthomieu, C. and R.J.P.r. Hienerwadel, *Fourier transform infrared (FTIR) spectroscopy*. (2009). **101**: p. 157-170.
- [75] Ojeda, J.J., M.J.M.S.B.M. Dittrich, and Protocols, *Fourier transform infrared spectroscopy for molecular analysis of microbial cells*. (2012): p. 187-211.
- [76] Inkson, B.J., *Scanning electron microscopy (SEM) and transmission electron microscopy (TEM) for materials characterization*, in *Materials characterization using nondestructive evaluation (NDE) methods*. (2016), Elsevier. p. 17-43.

- [77] Marturi, N., *Vision and visual servoing for nanomanipulation and nanocharacterization in scanning electron microscope*. (2013), Université de Franche-Comté.
- [78] Gopi, D., et al., *Evaluation of hydroxyapatite coatings on borate passivated 316L SS in Ringer's solution*. (2009). **29**(3): p. 955-958.
- [79] Sridhar, T., U.K. Mudali, and M.J.C.S. Subbaiyan, *Preparation and characterisation of electrophoretically deposited hydroxyapatite coatings on type 316L stainless steel*. (2003). **45**(2): p. 237-252.
- [80] Aksakal, B., et al., *The effect of coating thickness on corrosion resistance of hydroxyapatite coated Ti6Al4V and 316L SS implants*. (2010). **19**: p. 894-899.
- [81] Ekici, Ö., et al., *Evaluation of surface roughness after root resection: An optical profilometer study*. (2021). **84**(4): p. 828-836.
- [82] Wyant, J.C., et al., *An optical profilometer for surface characterization of magnetic media*. (1984). **27**(2): p. 101-113.
- [83] Park, S.-J. and M.-K. Seo, *Interface science and composites*. Vol. 18. (2011): Academic Press.
- [84] Leonova, L.A., E.L. Boytsova, and A.A. Pustovalova. *The study of titanium oxynitride coatings solubility deposited by reactive magnetron sputtering*. in *IOP Conference Series: Materials Science and Engineering*. (2016). IOP Publishing.
- [85] Bigi, A., et al., *Strontium-substituted hydroxyapatite nanocrystals*. (2007). **360**(3): p. 1009-1016.
- [86] Chandrasekar, A., S. Sagadevan, and A.J.I.J.P.S. Dakshnamoorthy, *Synthesis and characterization of nano-hydroxyapatite (n-HAP) using the wet chemical technique*. (2013). **8**(32): p. 1639-1645.
- [87] Pokhrel, S.J.A.i.C.E. and Science, *Hydroxyapatite: preparation, properties and its biomedical applications*. (2018). **8**(04): p. 225.
- [88] Salleh, A., et al., *The potential of silver nanoparticles for antiviral and antibacterial applications: A mechanism of action*. (2020). **10**(8): p. 1566.
- [89] Shirkhazadeh, M., M. Azadegan, and G.J.M.l. Liu, *Bioactive delivery systems for the slow release of antibiotics: incorporation of Ag⁺ ions into micro-porous hydroxyapatite coatings*. (1995). **24**(1-3): p. 7-12.

